43p.

CASE FILE COPY

N 62 14464

NASA TN D-1354

NASA TN D-1354

TECHNICAL NOTE

D-1354

AN EXPERIMENTAL AND ANALYTICAL INVESTIGATION OF THE NATURAL FREQUENCIES AND MODE SHAPES OF A FOUR-STAGE SOLID-PROPELLANT ROCKET VEHICLE

By Sumner A. Leadbetter, Vernon L. Alley, Jr.,
Robert W. Herr, and A. Harper Gerringer

Langley Research Center
Langley Station, Hampton, Va.

NATIONAL AERONAUTICS AND SPACE ADMINISTRATION
WASHINGTON

August 1962

NATIONAL AERONAUTICS AND SPACE ADMINISTRATION

TECHNICAL NOTE D-1354

AN EXPERIMENTAL AND ANALYTICAL INVESTIGATION OF THE NATURAL FREQUENCIES AND MODE SHAPES OF A FOUR-STAGE SOLID-PROPELLANT ROCKET VEHICLE

By Sumner A. Leadbetter, Vernon L. Alley, Jr.,
Robert W. Herr, and A. Harper Gerringer

SUMMARY

The results of a combined experimental and analytical investigation of the first three natural frequencies and mode shapes of a four-stage solid-propellant research vehicle are presented. A full-scale vehicle was assembled, with fuel mass simulated, and placed on a suspension system to simulate the free-free condition of flight. The agreement between the experimentally and analytically determined values for the mode shapes for all three modes and the natural frequency for the first mode was found to be very good. Differences of the order of 8 and 12 percent were noted between the calculated and measured values for the natural frequencies of the second and third modes, respectively.

The various stages of the vehicle were connected by screw-type joints and an experimental study was conducted to determine the effect of joint stiffness on the first natural frequency of the vehicle. This was done by unwinding individual joints between stages of the vehicle. The initial loosening of the joint between the second and third stages resulted in a 20-percent reduction of the first natural frequency. Further unscrewing of the joint did not cause further reduction of the frequency.

INTRODUCTION

The stabilization of multistage launch vehicles is usually accomplished either by spinning the vehicle about its longitudinal axis or by means of a closed-loop guidance system. With either method of stabilization, high dynamic stresses or structural failure may result from spin resonance or self-excited instabilities in which the natural free-free modes of the structure are pertinent parameters. If enough information about the mechanical characteristics of the vehicle is known to predict accurately the free-free body mode shapes and frequencies, the flight can be programed in such a manner that the forcing functions do

not excite the fundamental modes of the structure, and stable systems may be achieved. Since the structure of these vehicles is complex, combined experimental and analytical studies are desirable to ascertain the validity of analytically determined mode shapes and frequencies, particularly for inclusion of such effects as the stiffness and damping of the joints.

This report presents the results of a combined experimental and analytical investigation of the natural frequencies, mode shapes, and damping of a four-stage solid-propellant rocket vehicle. The fuel mass and fuel damping were simulated and the results of a study of the effects of joint stiffness are given.

SYMBOLS

A	matrix of equation (2), in./lb
c_u	coordinate to uth joint from m_o, in.
EI	stiffness coefficient of beam, lb-in.^{2}
h	distance between discrete masses, in.
L	total length of beam, in.
m	total mass of system, lb-sec^2/in.
m_j	jth discrete mass of p masses, lb-sec^2/in.
m_n	nth discrete mass, lb-sec^2/in.
m_o	mass at origin of z-coordinate system, lb-sec^2/in.
n	number of modes sought
p	number of discrete masses
r	radius of gyration of system about $\bar{z}$, in.
v	number of joints considered
x	coordinate along length of vehicle, in.
y_j	nth modal column (eigenfunction) for $j = 1$ to $p - 1$, in.

y_o deflection at m_o, in.

z coordinate from m_o, in.

$\bar{z}$ distance of center of gravity from center of gravity of m_o, in.

z_i coordinate to center of gravity of jth mass from center of gravity of m_o, in.

$\alpha_{i,j}$ portion of influence coefficient resulting from beam flexure only, in./lb

$\delta(u)_{i,j}$ contribution to influence coefficient due to local rotation of uth joint, in./lb

κ_u local rotation at c_u due to joint flexibility, radians/in-lb

λ eigenvalue of equation (2), in./lb

$\sigma_{i,j}$ deflection at i due to unit load at j when vehicle is considered cantilevered at $z = 0$, in./lb

ω_n nth natural circular frequency, radians/sec

Subscripts:

i, j, n, u integers

Matrix notations:

$\{\ \}$ column

$\lfloor\ \rceil$ diagonal

$[\ ]$ square

$\lfloor\ \rfloor$ row

$\lfloor 1 \rceil$ unit

APPARATUS AND TEST PROCEDURE

Description of Apparatus

Test vehicle.- The full-scale four-stage solid-propellant rocket vehicle shown in figure 1 was used as the test specimen. The vehicle was made up of the following rockets:

First stage	Lance
Second stage	Lance
Third stage	Recruit
Fourth stage	T55

All these rockets have been used, either individually or in combination, in aero-space research probes. A typical payload was attached at the top of the vehicle with mass to simulate the telemeter equipment. In order to simulate the condition of a vehicle during flight just prior to second-stage firing, an inert mass, having about the same density and stiffness as the solid fuel, was placed in the second and third stages. Concentrated masses were added to the fourth stage to simulate the fuel and instrumentation.

The interstage structural connection and separation device employed in this vehicle is a one piece, externally threaded, flanged bulkhead, generally referred to as a blowout diaphragm, and is shown in figure 2. The bulkhead and flange are radially slotted from the major diameter to the stiffened center portion of the bulkhead, forming a number of pie-shaped segments. The stages to be joined are provided with internal threads (6 to the inch) to match the bulkhead flange and assembled so that their circumferential mating surfaces are located at the approximate midpoint of the flange thread. A circumferential overlap or shear lip is included in the stage mating parts which maintains the shear capability of the skin. Preloading the threaded parts results in a juncture that behaves as a continuous member under both compressive and tensile loading. Stage separation is accomplished at ignition of the forward stage due to the pressure exerted by the rocket exhaust gases on the forward face of the bulkhead. With sufficient flange width, the circumferential segments initially react as a series of radial beams fixed at the flange end and free but guided at the stiffened center. The radial slots in the threaded flange allow the segments to pivot about the aft threads as the bulkhead deflection increases; this results in the release of the forward stage.

Test stand and shaker system.- One of the major problems encountered while determining the fundamental frequencies of a missile is the simulation of the free-free conditions of flight. The suspension system must

support the weight of the vehicle in such a manner that there is a minimum of interference with any vibratory body motion induced by oscillating forces applied to the vehicle. In the ideal case, the vehicle would be suspended in space without restraint in any direction. However, since this condition is not possible, a suspension system was set up in which the vehicle, when placed in the vertical attitude of flight, could approach freedom from restraint in one direction by supporting the vehicle weight by means of a lower clamp, located at or near a lower nodal point and stabilizing the vehicle in the upright position by supporting it by means of an upper clamp located at or near an upper nodal point.

A sketch of the test vehicle, indicating dimensions, weights, and centers of gravity, is shown in figure 3. The four stages were assembled, with approximately the same joint tightness as would be used during a launch, and placed on the suspension system. (See fig. 1.) The vehicle was suspended vertically with vertical cables attached to the lower clamps fastened on the first stage. Another set of horizontal cables, attached to the upper clamp on the third stage, was used to keep the vehicle from falling over. During the tests, the upper set of cables was loosened, and the vehicle was held by hand at the upper nodal point. A 50-pound vector-force electromagnetic exciter was connected to the vehicle at a point $10\frac{1}{2}$ inches from the bottom of the first stage, as shown in figure 4, to excite the normal modes in order to measure the mode shapes and frequencies. The locations of the suspension system clamps and the attachment point of the exciter are also indicated in figure 3.

Experimental Mode Shapes and Frequencies

The first three mode shapes and the corresponding frequencies of the vehicle were determined with the lower suspension support or clamp at two different station locations (tests 1 and 2, fig. 3) and with the vehicle rotated 90° about the axis of symmetry from the original condition (test 3). The latter test was conducted since the allowable tolerance in machining mating parts may cause unsymmetrical bending stiffness of the joints. Theoretically, in all aspects, the vehicle is designed to be symmetrical about the longitudinal axis. Further measurements were made to determine the effects of joint tightness and amplitude of oscillation on the frequency of the first natural mode with the vehicle suspended as during test 3.

In order to study the effects of joint tightness, vibration tests were made with the joint between the first and second stage unwound or loosened by increments to 20° (limited by the fins on the vehicle not clearing the supporting structure) and, after resetting this juncture to the original tightness, vibration tests were made with the joint

between the second and third stage unwound by increments to 80° of rotation. At both junctions, the stages separate at the rate of 0.00046 inch per degree of rotation. The accelerometer on the first stage nearest the exciter (accelerometer 1) was employed as the control instrument and was used to define the amplitude of oscillation.

Instrumentation

Eight strain-gage accelerometers were located along the length of the vehicle, two on each stage near the junctions, to measure displacements at the stations indicated in figure 3. The outputs from the accelerometers were fed through amplifiers to an oscillograph recorder for permanent records of the vibration data. The accelerometer data were reduced to obtain the natural frequencies, mode shapes, and structural damping of the vehicle. The accelerometers were attached to an adapter designed in such a manner that a cavity between the adapter and the vehicle could be evacuated with a vacuum pump to enable the accelerometer to be held in place by means of atmospheric pressure.

ANALYSIS

General Procedure

The first three natural modes of the subject vehicle were determined analytically by the matrix method for a discrete unsymmetrical mass system in free-free undamped natural oscillations given in reference 1. The resulting equations of motion are given by the following matrix equation:

$$\frac{1}{\omega_n^2 m}\{y_j\} = \left[[1] + \left[\frac{\bar{z}^2}{r^2}\left\{\frac{z_j}{\bar{z}}\right\}\left[1 - \frac{z_j}{\bar{z}}\right] - \{1\}\left[1 + \frac{\bar{z}^2}{r^2} - \frac{z_j}{\bar{z}}\frac{\bar{z}^2}{r^2}\right]\right]\left[\frac{m_j}{m}\right]\right]\left[\sigma_{i,j}\right]\left[\frac{m_j}{m}\right]\{y_j\} \qquad (1)$$

$$\begin{pmatrix} j = 1, 2, \ldots p - 1 \\ i = 1, 2, \ldots p - 1 \end{pmatrix}$$

where

y_j nth modal column (eigenfunction) for $j = 1$ to $p - 1$, in.

ω_n nth natural circular frequency, radians/sec

m total mass of system, lb-sec^2/in.

m_j jth discrete mass of p such masses, lb-sec^2/in.

z_j coordinate to center of gravity of jth mass from center of gravity of m_o, in.

$\bar{z}$ distance of center of gravity from center of gravity of m_o, in.

r radius of gyration of system about $\bar{z}$, in.

$\sigma_{i,j}$ deflection at i due to unit load at j when vehicle is considered cantilevered at z = 0, in./lb

$\{\}, [\ ], [\ ], [\ ], [1]$ column, diagonal, square, row, and unit matrices, respectively.

Equation (1) is a typical eigenvalue-eigenfunction equation of the sort

$$\lambda\{y_j\} = [A]\{y_j\} \tag{2}$$

and is solved by any one of a number of classical methods given in texts on matrix algebra, such as references 2 and 3. It should be noted in equation (1) that by choosing the origin of z at the center of gravity of m_o the order of the matrix was reduced from p to p - 1. This, however, results in the loss of y_o in the modal column which is shown in reference 1 to be

$$y_o = -\frac{m}{m_o}[1]\left[\frac{m_j}{m}\right]\{y_j\} \qquad (j = 1, 2, 3, \ldots p - 1) \tag{3}$$

Structural Parameters

Discrete masses.- The mass distribution for the subject vehicle is tabulated in table I and plotted as a function of x in figure 5. Note that the data presented in the table and figure are plotted on the x scale having its origin at the aftermost end of the vehicle. The z scale, applicable to the particular matrix solution of equation (1), has its origin at the zero discrete mass which for the test vehicle is at x = 13.36 inches. The discrete mass matrix solution for the analytically determined modes furnished herein was made by considering 31 lumped masses (p = 31). These masses and their locations are given in table II. Experience with this method in the solution of other related problems has

indicated that good results may be obtained by using $13\sqrt[3]{n}$ discrete masses where n, the number of the modes sought, is not greater than 5.

Influence coefficients.- The influence coefficients $\sigma_{i,j}$ used in equation (1) were computed by considering elementary beam flexure with the addition of local rotations due to joints. The influence coefficients were expressed in two parts:

$$\sigma_{i,j} = \alpha_{i,j} + \sum_{u=1}^{u=v} \delta(u)_{i,j} \tag{4}$$

where $\alpha_{i,j}$ is that portion of the influence coefficient resulting from beam flexure only and given by:

$$\alpha_{i,j} = \int_0^{z_i} \frac{z^2}{EI}\,dz - (z_j + z_i)\int_0^{z_i} \frac{z}{EI}\,dz + z_i z_j \int_0^{z_i} \frac{1}{EI}\,dz \qquad (j \geqq i) \tag{5}$$

$$\alpha_{i,j} = \alpha_{j,i} \qquad (j < 1)$$

and $\delta(u)_{i,j}$ is the contribution to the influence coefficient due to local rotation of the uth joint of which there are v joints. It is given by

$$\delta(u)_{i,j} = \kappa_u(z_j - c_u)(z_i - c_u) \qquad \left(z_j \geqq c_u \leqq z_i\right)$$

$$= 0 \qquad \left(z_j \leqq c_u \geqq z_i\right)$$

where

EI	stiffness coefficient of beam, lb-in.^{2}
z	coordinate from m_o, in.
c_u	coordinate to uth joint from m_o, in.
v	number of joints considered
κ_u	local rotation at c_u due to joint flexibility, radians/in-lb

Summing the contributions due to v-joints, adding to the bending coefficients, and utilizing Maxwell's reciprocal law, which is

$$\sigma_{i,j} = \sigma_{j,i}$$

provide a complete set of influence coefficients applicable to the specific problem.

The stiffness coefficients EI required in the above integrands are given in table II and figure 6 for the vehicle. The locations of the discrete masses (i and j) are listed in table III and the joint rotation constants are tabulated in table IV. A complete set of influence coefficients considering both flexure and joint influences is given as table V. These coefficients are references about a tangent at m_o - that is, the origin of the z coordinate system.

Joint rotation constants.- It has been observed in many rocket vehicles that significant local contributions to flexure frequently originate at joints and that these joint effects must be included in analyses involving flexure. The deflections generally defy rigorous analytical description. Such contributions are consistently encountered from looseness in screwed joints, thread deflections, flange flexibility, and plate and shell deformations that are not within the confines of beam theory. Since it is generally impractical to evaluate these effects analytically, the problem has been treated empirically at the Langley Research Center with satisfactory results in the determination of natural vibration characteristics. From limited measurements and observations of the inordinate behavior of typical rocket-vehicle joints, the order of magnitude of rotations resulting from moment loading are called joint rotation constants. These constants κ_u are defined as the measure of the local rotation of the structure due to the application of bending moment and are measured in radians/in-lb.

Admittedly, many typical local deflections are highly inordinate and nonlinear and for such cases the linear empirical approach can only hope to provide an equivalent effect. Also, experience has shown that considerable variation in the behavior of similar joint designs can result from variation in fabrication skill. However, it should be kept in mind that estimates of κ_u are approximations to what should normally be a secondary influence in a good design, and it is upon this premise that such empirical means have been employed resulting in consistently improved accuracy of modal data. Invariably, computed mode data on rocket vehicles that disregard such local influences will result in frequencies higher than actual; therefore, any reasonable approximation to joint behavior will move the computed results in the proper direction. Nevertheless, the possibility of assuming joint factors unreasonably large does exist and consequently such efforts may result in greater errors than would be experienced if totally ignored.

A guide to joint evaluation which should provide a simple means for approximating the joint rotation constants in a typical rocket vehicle is shown in figure 7 where a variety of typical rocket-vehicle joints are illustrated and classified from excellent to poor in light of their stiffness. Repeated experiences with bending resulting from local joint rotations has led to the classification shown. The curves of figure 7 were drawn from 10 measured quantities of κ_u for a variety of different classes of joints. Because of the limited quantity of measured data the curves which show the variation in κ_u with diameter were not empirically established but were based on the assumption that κ_u is inversely proportional to the third power of the diameter. This assumption is in accordance with the theoretical variation in flexibility of geometrically similar joints and the resulting curves proved to be in good agreement with the measured data. Information of the type given in figure 7 is primarily useful to designers who repeatedly utilize the same types of joints in a variety of rocket-vehicle assemblies.

It is improbable that the factors contributing to so-called joint rotation effects will ever be amenable to thorough analytical treatment; this leaves two major avenues of approach to the solution: first and perhaps most appropriate, to design structures that will avoid most of the geometries which defy analysis and permit inordinate behaviors, and second and as a last resort, to use empirical joint rotation data such as those given in figure 7 for various classes of fabrications.

The data of figure 7 are from limited observations, and considerable improvement in this approach should result from a finer classification of hardware and from a greatly increased sampling of joint data.

Significance of joints on the subject vehicle.- The contributions of $\alpha_{i,j}$ and $\delta(u)_{i,j}$ to the influence coefficients are illustrated for a specific case. In table V the total influence coefficient $\sigma_{i,j}$ for $i = 25$ and $j = 29$ is 0.01755 in./lb.

The contribution due to elementary beam flexure is

$$\alpha_{25,29} = 0.01721$$

and the contributions due to the first four joints (u = 1, 2, 3, and 4) are:

$$\sum_{u=1}^{u=v} \delta(u)_{i,j} = 1.78 \times 10^{-9}(373.16)(341.15) + 1.78 \times 10^{-9}(185.61)(153.60)$$

$$+ 11.00 \times 10^{-9}(68.54)(36.53) + 25.00 \times 10^{-9}(53.16)(21.15)$$

$$= 0.00023 + 0.00005 + 0.00003 + 0.00003$$

$$= 0.00034 \text{ in./lb}$$

See tables III and IV.

The fifth joint does not contribute since:

$$c_{u=5} > z_{i=25}$$

The numbers in the previous calculations show that the joints increase the influence coefficient $\alpha_{25,29}$ due to ordinary bending by 2.0 percent. A similar comparison for $i = j = 30$ shows a 6.7-percent increase in $\alpha_{30,30}$ due to joint contributions. All joints except the 5th joint $\left(\kappa_u = 900 \times 10^{-9}\right)$ are considered as high quality junctures and do not materially influence the flexure of the vehicle. In vehicles with low quality joints, the increases in the influence coefficients are generally well above those noted in the aforementioned examples. A comparison of the first three natural frequencies with and without joint considerations shows increases of 1.8 percent, 4.5 percent, and 11.5 percent in the first, second, and third modes, respectively, when omitting the joint effects.

Secondary influences of rotary inertia and shear deformation.- The equation for natural modes (eq. (1)) cannot accommodate the secondary influence of rotary inertia. However, the secondary contribution of shear deformation can be easily added by the simple addition of such effects to the influence coefficients. In the calculated modes (curves labeled theory in figs. 8, 9, and 10) the effects of shear and rotary inertia were not considered. The discrepancies between calculated and measured results noted in the second and third modes can in part be attributed to this omission.

Example of Analytical Procedure

An illustration of the application of the frequency equation (eq. (1)) for an elementary model is submitted to aid the reader in the

interpretation and utilization of the equations. The following analogy consists of a beam of uniform mass and stiffness treated as a system of four discrete masses as shown in the following sketch:

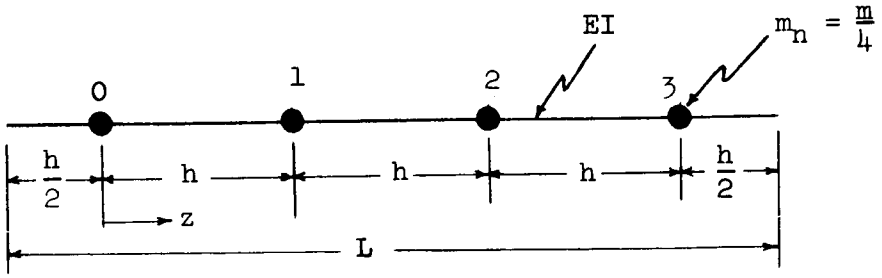

The basic quantities $\bar{z}$, r, and m_n are readily found for the uniform system as

$$\bar{z} = \frac{\sum_{n=0}^{p-1} m_n z_n}{\sum_{n=0}^{p-1} m_n} = \frac{\sum_{n=0}^{3} hn}{4} = \frac{3}{2} h$$

$$r^2 = \frac{\sum_{n=0}^{p-1} m_n z_n^2}{\sum_{n=0}^{p-1} m_n} - \bar{z}^2 = \frac{\sum_{n=0}^{3} h^2 n^2}{4} - \bar{z}^2 = \frac{14}{4} h^2 - \frac{9}{4} h^2 = \frac{5}{4} h^2$$

$$m_n = \frac{m}{4}$$

The various column matrices are then

$$\begin{Bmatrix} z_j \\ \bar{z} \end{Bmatrix} = \frac{2}{3} \begin{Bmatrix} 1 \\ 2 \\ 3 \end{Bmatrix}$$

$$\left\{1 - \frac{z_j}{\bar{z}}\right\} = \frac{1}{3}\begin{Bmatrix} 1 \\ -1 \\ -3 \end{Bmatrix}$$

$$\left\{1 + \frac{\bar{z}^2}{r^2} - \frac{z_j}{\bar{z}}\frac{\bar{z}^2}{r^2}\right\} = \frac{1}{5}\begin{Bmatrix} 8 \\ 2 \\ -4 \end{Bmatrix}$$

The mass ratio diagonal matrix is

$$\left[\frac{m_j}{m}\right] = \frac{1}{4}\begin{bmatrix} 1 & & \\ & 1 & \\ & & 1 \end{bmatrix}$$

If the column matrices are utilized, the square matrix of the z and r terms becomes

$$\left[\frac{2}{5}\begin{bmatrix} 1 & -1 & -3 \\ 2 & -2 & -6 \\ 3 & -3 & -9 \end{bmatrix} - \frac{1}{5}\begin{bmatrix} 8 & 2 & -4 \\ 8 & 2 & -4 \\ 8 & 2 & -4 \end{bmatrix}\right] = -\frac{2}{5}\begin{bmatrix} 3 & 2 & 1 \\ 2 & 3 & 4 \\ 1 & 4 & 7 \end{bmatrix}$$

Multiplying these matrices by the diagonal matrix $\left[m_j/m\right]$ and adding the results to the identity matrix $[1]$ yield the premultiplier of the matrix $\left[\sigma_{i,j}\right]$; that is

$$\left[[1] + \left[\frac{\bar{z}^2}{r^2}\left\{\frac{z_j}{\bar{z}}\right\}\left[1 - \frac{z_j}{\bar{z}}\right] - \{1\}\left[1 + \frac{\bar{z}^2}{r^2} - \frac{z_j}{\bar{z}}\frac{\bar{z}^2}{r^2}\right]\right]\left[\frac{m_j}{m}\right]\right] = \frac{1}{10}\begin{bmatrix} 7 & -2 & -1 \\ -2 & 7 & -4 \\ -1 & -4 & 3 \end{bmatrix}$$

Since EI is assumed constant, the development of the influence coefficient matrix is as follows

$$\alpha_{i,j} = \frac{h^3}{EI}\left[\int_0^{n=i} n^2 dn - (j+i)\int_0^{n=i} n\,dn + ij\int_0^{n=i} dn\right] \qquad (z = hn)$$

$$\alpha_{i,j} = \frac{h^3}{EI}\left[\frac{i^3}{3} - (j+i)\frac{i^2}{2} + i^2 j\right] = \frac{h^3}{EI} i^2\left(\frac{j}{2} - \frac{i}{6}\right) \qquad (j \geqq i)$$

$$\alpha_{1,1} = \frac{h^3}{EI}\frac{1}{3} \qquad \alpha_{2,2} = \frac{h^3}{EI}\frac{8}{3}$$

$$\alpha_{1,2} = \frac{h^3}{EI}\frac{5}{6} = \alpha_{2,1} \qquad \alpha_{2,3} = \frac{h^3}{EI}\frac{14}{3} = \alpha_{3,2}$$

$$\alpha_{1,3} = \frac{h^3}{EI}\frac{8}{6} = \alpha_{3,1} \qquad \alpha_{3,3} = \frac{h^3}{EI}9$$

From the above computations, the influence coefficients due to simple flexure are stated as follows:

$$\alpha_{i,j} = \frac{1}{6}\frac{h^3}{EI}\begin{bmatrix} 2 & 5 & 8 \\ 5 & 16 & 28 \\ 8 & 28 & 54 \end{bmatrix}$$

Assume also a joint of flexibility κ_1 at $z_u = h$, then the contributions to the overall influence coefficients are

$$\delta_{i,j} = \kappa_1 h^2 (j-1)(i-1) \qquad (j \geqq 1 \geqq i)$$

$$\delta_{1,1} = \kappa_1 h^2(0) \qquad \delta_{2,2} = \kappa_1 h^2$$

$$\delta_{1,2} = \kappa_1 h^2(0) \qquad \delta_{2,3} = \kappa_1 h^2 2 = \delta_{3,2}$$

$$\delta_{1,3} = \kappa_1 h^2(0) \qquad \delta_{3,3} = \kappa_1 h^2 4$$

Thus the matrix $\delta_{i,j}$ for the one joint becomes

$$\delta_{i,j} = \kappa_1 h^2 \begin{bmatrix} 0 & 0 & 0 \\ 0 & 1 & 2 \\ 0 & 2 & 4 \end{bmatrix}$$

Adding the $\alpha_{i,j}$ and $\delta_{i,j}$ matrices together yields the total influence coefficient matrix $\sigma_{i,j}$ for the system with the joint. Rather than complicate the remaining illustration it is expedient to omit the joint contribution, and a general solution of the four-mass system can then be given. The frequency equation becomes

$$\frac{1}{\omega_n^2 m} \{y_j\} = \frac{1}{10} \begin{bmatrix} 7 & -2 & -1 \\ -2 & 7 & -4 \\ -1 & -4 & 3 \end{bmatrix} \frac{h^3}{6EI} \begin{bmatrix} 2 & 5 & 8 \\ 5 & 16 & 28 \\ 8 & 28 & 54 \end{bmatrix} \frac{1}{4} \begin{bmatrix} 1 & & \\ & 1 & \\ & & 1 \end{bmatrix} \{y_j\}$$

$$\frac{EI}{\omega_n^2 m L^3} \{y_j\} = \frac{1}{15360} \begin{bmatrix} -4 & -25 & -54 \\ -1 & -10 & -36 \\ 2 & 15 & 42 \end{bmatrix} \{y_j\}$$

Solving by matrix iteration for the lowest frequency gives

$$\frac{15360EI}{\omega^2 m L^3} = 25 \qquad \{y_j\} = \begin{Bmatrix} -1 \\ -1 \\ 1 \end{Bmatrix} \qquad (j = 1, 2, \text{ and } 3)$$

$$\omega = 24.79\sqrt{\frac{EI}{mL^3}} \qquad f = 3.95\sqrt{\frac{EI}{mL^3}} \qquad (y_o = 1)$$

The first-mode frequency computed for the analogous four-mass system is 11 percent higher than the exact solution for a symmetrical uniform beam

in free-free vibration. This example is given to illustrate the operations in extending the frequency equation and is not for the purpose of estimating frequencies. However, the agreement with the exact solution is considered good in view of the crude analogy given by the four masses. Doubling the number of masses will reduce the 11-percent error to 2.5 percent. Tripling the number of masses will reduce the error to 1 percent. In any case, inherently, the computed frequency will be higher than the actual frequency for discrete mass solutions of the type presented.

RESULTS AND DISCUSSION

Presentation of Results

The results of the experimental measurements and the analytical study of the first three normal mode shapes and frequencies are presented in figures 8, 9, and 10. The inputs for the analyses are given in tables I to V. Other experimental results, including a study of the effect of joint looseness and amplitude of oscillation, are presented in figures 11, 12, and 13, and a sampling of damping coefficients is given in table VI.

The analytically determined mode shapes are indicated by the solid curve and the normalized experimentally measured deflections are presented as data points. Also shown in figures 8, 9, and 10 are the experimentally and the analytically determined natural frequencies.

The damping coefficient, defined as the ratio of twice the viscous damping to the critical damping, was measured from the outputs of the accelerometers. They are, in general, of the expected magnitude.

Comparison of Experimental and Analytical Results

The results of the experimental and analytical studies of the first three normal body modes are presented in figures 8, 9, and 10. The results show that the mode shapes for the first mode, as determined experimentally, are in excellent agreement with the results of the analytical study for all test conditions; and that the analysis adequately predicts the mode shapes of the second and third free-free modes with some small deviations of the deflection curve at the upper stages of the vehicle. The magnitude of the drive force and the location of the support clamp had no appreciable effect on the first-mode shape, but caused a slight variation of the mode shapes for the higher modes - the third mode in particular.

The average of the first-mode frequencies for all the cases measured and shown in figure 8 differed from the calculated frequency by about 1 percent which is within the accuracy of the measured data. The frequency of the vehicle for the same support position but with the rocket rotated 90° about its longitudinal axis was within about 2 percent of the calculated value. The vehicle was supposedly symmetrical about the longitudinal axis and the difference between test 2 and test 3 indicates the possible variations in frequency resulting from unavoidable fabrication and machining effects. The observed variation in frequency suggests that the ability to predict first-mode frequencies may be limited in accuracy by the quality control of the structure.

The results of the experimental and analytical study of the second-mode shape and frequency are presented in figure 9. The analysis adequately predicts the mode shape but the calculated frequency is about 8 percent higher than the average of the measured values. In the experimental study, there was a spread of 4 percent in the measured second-mode natural frequencies attributed to measurement techniques, structural inconsistencies, and nonlinearities of the system. The second-mode tests supported the findings in the first-mode studies of different vibration characteristics for motions in longitudinal planes normal to each other. A 3-percent reduction in second-mode frequency was observed in test 3 for the vehicle rotated 90° about its longitudinal axis.

The results of the experimental and analytical study of the third-mode shape and frequency are presented in figure 10. For the results shown in this figure for the test 1 configuration there was a noticeable variation between the measured and calculated mode shapes in the upper stage of the vehicle; however, very good agreement was observed over the total length in tests 2 and 3. The third mode was the only mode that exhibited a significant sensitivity to the location of the lower support position. A shift in third-mode frequency of approximately 6 percent was attributed to changing the lower support location. It was consistently observed that all modes displayed decreases in frequency as the lower support position was moved toward the nodal points of the modes. The measured frequency of the third mode varied from 7 to 25 percent lower than the calculated value with an average variation of 12 percent from the calculated for all the third-mode measured frequencies. The lack of symmetry for oscillations in longitudinal planes normal to each other was quite apparent in the third mode. A 12-percent reduction in the third-mode frequency was recorded in the configuration designated as test 3 where the excitation of the vehicle was normal to the test plane of tests 1 and 2. The reduction in frequency for motions in the 90° plane was consistent with all three modes. It is appropriate, at this point, to discuss some of the errors that may be involved in the studies.

The high length-to-diameter ratio of the test vehicle implements the belief that, for the three modes investigated, rotary inertia and shear omissions in the calculations could hardly account for the differences observed in the frequencies of the second and third modes. An analytical study to determine the significance of rotary inertia and shear deformation revealed that their inclusion would amount to a 0.4-, 1.5-, and 1.9-percent reduction in the calculated first-, second-, and third-mode frequencies, respectively. Furthermore, the errors introduced by the process of lumping the masses are unlikely the source since such effects should be well below 1 percent. The previously mentioned rule $13\sqrt[3]{n}$ for determining the number of masses compatible with a 1-percent error indicated that 19 masses would have been sufficient for controlling errors to within 1 percent. The 31 masses used in the analysis should introduce errors of less than 1 percent due to the discrete representation of the continuous system.

It then remains that the frequency errors are most logically attributed to the inadequate representation of the vehicle's stiffness properties. This is a reasonable expectancy in light of the extreme complexity of the structure of a typical space vehicle and will always be a fertile source of error that will vary considerably with the skill and intuition of the analyst. No generalization can be made as to the influence on the various modes of inadequate geometric representation, since the significance of such discrepancies on a given mode depends strongly upon the location of such errors. For instance, an overlooked region of flexibility will not alter the frequency of the mode if it coincides with, or is near, an inflection point, but it can have a large effect on another mode where such favorable conditions do not exist.

It should also be noted that complicated structures of the same type as the test vehicle frequently exhibit a degree of flexural nonlinearity. In comparing the measured results with the results of calculations based on an assumed linear system, the best agreements are generally to be expected for the lowest amplitudes of oscillations. No strong correlation of this nature can be drawn, however, from the results of the tests reported herein, since the different levels of excitation effected increases in frequency with increases in driving forces in some cases and reduction in frequency in others. This inordinate behavior of the frequency variation with driving forces is indicated primarily in figure 9. However, from the data presented in figure 12, with looseness existing in joint, the frequency-amplitude relationship appears to be of the expected behavior. The decrease in frequency with increase in the amplitude of oscillation for the low level vibration is in agreement with the behavior of some nonlinear systems. Another indication of a nonlinear system was exhibited, in tuning the system to a particular mode, by a jump from a high amplitude of oscillation to a lower amplitude as the frequency was varied. Care was taken in tuning the system to obtain the maximum amplitude of oscillations.

Effects of Joint Looseness

Looseness of the screw joint between the first and second stages affected the first natural frequency as indicated in figure 11. As the amplitude of oscillation (measured by the accelerometer nearest the exciter) is increased, the natural frequency at first decreases and then increases. In contrast, the natural frequency of a single-degree-of-freedom system with free play approaches zero at small amplitudes and increases with amplitude. In the present case, for small amplitudes of oscillation, the mass of the upper stages holds the screw threads firmly in contact throughout a cycle and the natural frequency is therefore essentially the same as for a tight joint. At larger amplitudes of oscillation the joint is rocking back and forth through the free play of the threads and thus displays nonlinearities analogous to the single-degree-of-freedom system with free play.

The data obtained while unwinding the joint between the second and third stages are presented in figure 12. Again the frequency tends to decrease and then increase as the amplitude of oscillation is increased.

A plot of frequency as a function of degrees of rotation or unwinding at constant amplitude of oscillation is presented in figure 13. The results of unwinding the joint between the first and second stages are shown in figure 13(a) and the results of unwinding the joint between the second and third stages are shown in figure 13(b). The results indicate that the frequency is reduced, with an amplitude of oscillation of 0.30 inch, by about 36 percent when the joint is unwound 30°. A smaller variation in frequency is noted for lesser amplitudes of oscillation. There is not much frequency variation at the low displacement level throughout the test region of unwinding. In figure 13(b) for a displacement of 0.10 inch, there is a reduction in frequency of about 8 percent at about 15° of rotation and then the frequency tends to increase. For an oscillatory displacement of 0.30 inch, the frequency decreases by about 20 percent until the stages are unwound to about 30° and then essentially remains constant. It should be pointed out that the same trends were observed when unwinding either the joint between the first and second stage or unwinding the joint between the second and third stage. These characteristics are probably a function of the characteristics of the threads and the attitude in which the missile is supported.

CONCLUSIONS

As a result of the experimental and analytical investigation of the vibration characteristics of a four-stage solid-propellant rocket vehicle reported herein, the following conclusions can be made:

1. The results show that the natural frequency measured for the first mode is in excellent agreement with the results obtained by the analytical procedure outlined herein. The calculated frequency for the second mode is about 8 percent higher than the measured value, whereas the calculated frequency for the third mode varies from 7 percent to 25 percent higher than the measured values.

2. The analytical procedure presented adequately predicted the mode shapes of the first three modes.

3. The location of the suspension system clamp on the vehicle, in relation to the nodal points, did not appreciably affect the free-free natural mode shapes and caused only small differences in the natural frequencies.

4. The structure, although intended to be geometrically symmetrical about the longitudinal axis, exhibits a small but consistent difference in the vibration characteristics of the first three modes for test in longitudinal planes 90° with respect to each other. The unsymmetrical behavior indicates that the inherent influences of tolerances and fabrication effects might produce unpredictable variations in frequencies of several percent in two theoretically similar vehicles.

5. Reductions in the natural frequencies of the first mode of up to 20 percent were noted during initial unwinding of the screw joints between the first and second stages and the second and third stages. The natural frequency of the vehicle tended to decrease with initial unwinding of a screw joint between stages and then either increase slightly or remain constant within the scope of the experimental program.

6. It is believed that the differences between measured and computed frequencies are due primarily to the differences between the actual mass and stiffness of the vehicle and the corresponding values used in the computations. These parameters are subject to variations for a complicated structure of the type tested due to the individual interpretation of the structural properties.

Langley Research Center,
National Aeronautics and Space Administration,
Langley Station, Hampton, Va., March 30, 1962.

REFERENCES

1. Alley, Vernon L., Jr., and Gerringer, A. Harper: A Matrix Method for the Determination of the Natural Vibrations of Free-Free Unsymmetrical Beams With Application to Launch Vehicles. NASA TN D-1247, 1962.

2. Frazer, R. A., Duncan, W. J., and Collar, A. R.: Elementary Matrices. Cambridge Univ. Press, 1950.

3. Michal, Aristotle D.: Matrix and Tensor Calculus. John Wiley & Sons, Inc., c.1947.

TABLE I.- MASS DISTRIBUTION OF TEST VEHICLE

Span of x, in.	Mass per inch, m_x, lb-sec^2/in.^{2}
0 to 13.36	0.016666
13.36 to 20.83	.029350
20.83 to 180.80	.0058238
180.80 to 187.62	.021653
187.62 to 199.51	.016666
199.51 to 208.47	.029350
208.47 to 287.94	.025956
287.94 to 368.42	.025311
368.42 to 375.14	.014746
375.14 to 387.13	.0041010
387.13 to 396.41	.010091
396.41 to 444 22	.0086943
444.22 to 486.32	.011212
486.32 to 492.22	.0076917
492.22 to 500.42	.0020933
500.42 to 507.62	.0027176
507.62 to 521.77	.0046477
521.77 to 535.62	.0048523
535.62 to 544.07	.0041425
544.07 to 553.11	.0036010
553.11 to 557.92	.0020244
[a]558.42	.0011748
[a]560.92	.00049260
560.92 to 562.42	.0032480
562.42 to 562.67	.00089973
565.13	.0014562
[a]567.13	.0024100
[a]569.13	.0034100
571.63	.0045250

[a]The m_x function is continuous but not constant between x = 557.92 to 560.92 and between 562.67 and 571.63. In these regions the span listings are not applicable and point listing has been used.

TABLE II.- FLEXURAL STIFFNESS DISTRIBUTION OF TEST VEHICLE

x, in.	EI, lb-in.^{2}	x, in.	EI, lb-in.^{2}	x, in.	EI, lb-in.^{2}
0	1.4850 $\times 10^9$	369.94	1.39676 $\times 10^9$	506.02	0.039150 $\times 10^9$
17.87	1.4850	371.54	1.49527	502.27	.026100
19.87	2.4200	373.34	1.63490	506.52	.028768
20.37	8.5800	374.51	2.68879	507.02	.034481
20.87	8.5800	375.23	3.68237	507.52	.040229
21.87	11.71166	375.82	2.98879	507.92	.069107
22.87	8.87083	376.62	2.83245	508.70	.093061
23.87	6.78481	380.62	2.13201	509.17	.055245
25.07	4.25204	384.62	1.55777	509.32	.10582
176.62	4.25204	388.62	1.09721	531.62	.11052
177.72	6.78711	392.27	.80000	534.07	.024684
178.72	8.87083	392.62	.73780	535.17	.17783
179.72	11.71166	395.91	.50907	535.62	.59584
181.23	6.31804	396.41	.47247	535.92	.39576
183.62	2.67801	396.41	.96480	536.62	.056400
186.22	4.89397	397.16	.96480	537.57	.056400
187.02	9.03489	397.54	1.34402	537.72	.21435
187.62	2.64768	398.39	.58306	538.27	.21435
188.22	10.11358	486.32	.58306	539.42	.16049
189.22	3.78030	486.32	.34272	539.84	.040637
193.55	3.59161	487.62	.34272	553.02	.040637
198.04	2.50320	489.27	.19994	553.22	.081120
198.39	3.38400	490.22	.34272	554.515	.081120
205.69	3.38400	490.52	.29809	554.86	.22789
206.89	4.06552	491.52	1.33336	555.61	.22789
207.45	6.99076	491.87	.23341	557.86	.10737
208.45	8.39440	492.22	.12491	561.035	.01360
209.45	10.59940	492.62	.20857	561.36	.013134
210.45	8.87083	492.97	.24705	561.36	.046854
211.45	6.27585	500.42	.21425	562.86	.046854
212.62	4.25257	501.92	.098572	562.86	.0035952
364.22	4.25257	502.92	.076502	563.11	.0035952
365.42	6.80383	503.92	.053592	563.11	.0014726
366.42	8.87083	504.92	.030827	568.70	.0014726
367.42	11.72498	505.52	.044950		
368.82	1.33614	505.92	.049300		

TABLE III.- STATION LOCATIONS AND EQUIVALENT DISCRETE MASSES

[L = 571.63; z = 0 is located at x = 13.36 $\left(x_o/L = 0.02337\right)$; $z_i = L\left(x_i/L\right) - 13.36$]

i or j	x_i/L or x_j/L	m_i, lb-sec^2/in.	i or j	x_i/L or x_j/L	m_i, lb-sec^2/in.
0	0.0234	0.44811	16	0.707	0.13859
1	.0596	.15433	17	.735	.13859
2	.106	.15433	18	.763	.13859
3	.152	.15433	19	.789	.15731
4	.199	.15620	20	.814	.15731
5	.247	.15620	21	.838	.15731
6	.293	.15620	22	.856	.045381
7	.347	.60939	23	.875	.036732
8	.388	.68757	24	.900	.065765
9	.434	.68757	25	.925	.067205
10	.481	.68757	26	.944	.034963
11	.527	.67909	27	.960	.032589
12	.574	.67909	28	.970	.0085982
13	.621	.67909	29	.981	.0084114
14	.656	.20564	30	.995	.020500
15	.686	.083551			

TABLE IV.- JOINT ROTATION CONSTANTS

Joint No., u	Joint location, x/L	Joint rotation constant, κ_u, radians/in-lb
1	0.3282	1.78×10^{-9}
2	.6563	1.78
3	.8611	11.000
4	.8880	25.000
5	.9376	900.000

TABLE V.- INFLUENCE COEFFICIENTS

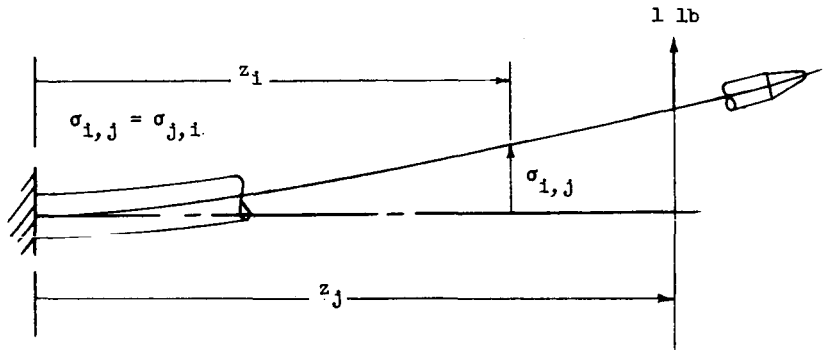

i,j	$\sigma_{i,j}$, in./lb	i,j	$\sigma_{i,j}$, in./lb	i,j	$\sigma_{i,j}$, in./lb
1, 1	0.8430×10^{-5}	2, 3	0.6140×10^{-4}	3, 6	0.2226×10^{-3}
1, 2	$.1738 \times 10^{-4}$	2, 4	$.8388 \times 10^{-4}$	3, 7	$.2695 \times 10^{-3}$
1, 3	$.2632 \times 10^{-4}$	2, 5	$.1065 \times 10^{-3}$	3, 8	$.3049 \times 10^{-3}$
1, 4	$.3532 \times 10^{-4}$	2, 6	$.1292 \times 10^{-3}$	3, 9	$.3450 \times 10^{-3}$
1, 5	$.4437 \times 10^{-4}$	2, 7	$.1553 \times 10^{-3}$	3, 10	$.3852 \times 10^{-3}$
1, 6	$.5344 \times 10^{-4}$	2, 8	$.1750 \times 10^{-3}$	3, 11	$.4255 \times 10^{-3}$
1, 7	$.6390 \times 10^{-4}$	2, 9	$.1974 \times 10^{-3}$	3, 12	$.4662 \times 10^{-3}$
1, 8	$.7177 \times 10^{-4}$	2, 10	$.2197 \times 10^{-3}$	3, 13	$.5068 \times 10^{-3}$
1, 9	$.8072 \times 10^{-4}$	2, 11	$.2422 \times 10^{-3}$	3, 14	$.5375 \times 10^{-3}$
1, 10	$.8966 \times 10^{-4}$	2, 12	$.2649 \times 10^{-3}$	3, 15	$.5633 \times 10^{-3}$
1, 11	$.9865 \times 10^{-4}$	2, 13	$.2875 \times 10^{-3}$	3, 16	$.5817 \times 10^{-3}$
1, 12	$.1077 \times 10^{-3}$	2, 14	$.3046 \times 10^{-3}$	3, 17	$.6058 \times 10^{-3}$
1, 13	$.1168 \times 10^{-3}$	2, 15	$.3189 \times 10^{-3}$	3, 18	$.6300 \times 10^{-3}$
1, 14	$.1236 \times 10^{-3}$	2, 16	$.3292 \times 10^{-3}$	3, 19	$.6527 \times 10^{-3}$
1, 15	$.1293 \times 10^{-3}$	2, 17	$.3426 \times 10^{-3}$	3, 20	$.6739 \times 10^{-3}$
1, 16	$.1334 \times 10^{-3}$	2, 18	$.3561 \times 10^{-3}$	3, 21	$.6952 \times 10^{-3}$
1, 17	$.1388 \times 10^{-3}$	2, 19	$.3687 \times 10^{-3}$	3, 22	$.7103 \times 10^{-3}$
1, 18	$.1442 \times 10^{-3}$	2, 20	$.3805 \times 10^{-3}$	3, 23	$.7272 \times 10^{-3}$
1, 19	$.1492 \times 10^{-3}$	2, 21	$.3924 \times 10^{-3}$	3, 24	$.7488 \times 10^{-3}$
1, 20	$.1540 \times 10^{-3}$	2, 22	$.4008 \times 10^{-3}$	3, 25	$.7700 \times 10^{-3}$
1, 21	$.1587 \times 10^{-3}$	2, 23	$.4102 \times 10^{-3}$	3, 26	$.7869 \times 10^{-3}$
1, 22	$.1621 \times 10^{-3}$	2, 24	$.4223 \times 10^{-3}$	3, 27	$.8002 \times 10^{-3}$
1, 23	$.1659 \times 10^{-3}$	2, 25	$.4341 \times 10^{-3}$	3, 28	$.8092 \times 10^{-3}$
1, 24	$.1707 \times 10^{-3}$	2, 26	$.4435 \times 10^{-3}$	3, 29	$.8190 \times 10^{-3}$
1, 25	$.1754 \times 10^{-3}$	2, 27	$.4508 \times 10^{-3}$	3, 30	$.8307 \times 10^{-3}$
1, 26	$.1792 \times 10^{-3}$	2, 28	$.4559 \times 10^{-3}$		
1, 27	$.1821 \times 10^{-3}$	2, 29	$.4614 \times 10^{-3}$	4, 4	$.2033 \times 10^{-3}$
1, 28	$.1841 \times 10^{-3}$	2, 30	$.4678 \times 10^{-3}$	4, 5	$.2665 \times 10^{-3}$
1, 29	$.1863 \times 10^{-3}$			4, 6	$.3299 \times 10^{-3}$
1, 30	$.1889 \times 10^{-3}$	3, 3	$.1008 \times 10^{-3}$	4, 7	$.4029 \times 10^{-3}$
		3, 4	$.1412 \times 10^{-3}$	4, 8	$.4579 \times 10^{-3}$
2, 2	$.3903 \times 10^{-4}$	3, 5	$.1819 \times 10^{-3}$	4, 9	$.5203 \times 10^{-3}$

TABLE V.- INFLUENCE COEFFICIENTS - Continued

i, j	$\sigma_{i,j}$, in./lb	i, j	$\sigma_{i,j}$, in./lb	i, j	$\sigma_{i,j}$, in./lb	i, j	$\sigma_{i,j}$, in./lb	i, j	$\sigma_{i,j}$, in./lb	i, j	$\sigma_{i,j}$, in./lb
4, 10	0.5828×10^{-3}	5, 15	0.1205×10^{-2}	6, 21	0.1991×10^{-2}	7, 28	0.3090×10^{-2}	9, 14	0.2841×10^{-2}	10, 24	0.4884×10^{-2}
4, 11	$.6456 \times 10^{-3}$	5, 16	$.1246 \times 10^{-2}$	6, 22	$.2036 \times 10^{-2}$	7, 29	$.3130 \times 10^{-2}$	9, 15	$.2999 \times 10^{-2}$	10, 25	$.5040 \times 10^{-2}$
4, 12	$.7088 \times 10^{-3}$	5, 17	$.1300 \times 10^{-2}$	6, 23	$.2087 \times 10^{-2}$	7, 30	$.3178 \times 10^{-2}$	9, 16	$.3111 \times 10^{-2}$	10, 26	$.5164 \times 10^{-2}$
4, 13	$.7721 \times 10^{-3}$	5, 18	$.1354 \times 10^{-2}$	6, 24	$.2152 \times 10^{-2}$			9, 17	$.3259 \times 10^{-2}$	10, 27	$.5262 \times 10^{-2}$
4, 14	$.8197 \times 10^{-3}$	5, 19	$.1404 \times 10^{-2}$	6, 25	$.2216 \times 10^{-2}$	8, 8	$.1218 \times 10^{-2}$	9, 18	$.3407 \times 10^{-2}$	10, 28	$.5328 \times 10^{-2}$
4, 15	$.8599 \times 10^{-3}$	5, 20	$.1452 \times 10^{-2}$	6, 26	$.2267 \times 10^{-2}$	8, 9	$.1418 \times 10^{-2}$	9, 19	$.3545 \times 10^{-2}$	10, 29	$.5401 \times 10^{-2}$
4, 16	$.8884 \times 10^{-3}$	5, 21	$.1499 \times 10^{-2}$	6, 27	$.2307 \times 10^{-2}$	8, 10	$.1618 \times 10^{-2}$	9, 20	$.3675 \times 10^{-2}$	10, 30	$.5487 \times 10^{-2}$
4, 17	$.9260 \times 10^{-3}$	5, 22	$.1533 \times 10^{-2}$	6, 28	$.2334 \times 10^{-2}$	8, 11	$.1819 \times 10^{-2}$	9, 21	$.3806 \times 10^{-2}$		
4, 18	$.9636 \times 10^{-3}$	5, 23	$.1570 \times 10^{-2}$	6, 29	$.2364 \times 10^{-2}$	8, 12	$.2021 \times 10^{-2}$	9, 22	$.3898 \times 10^{-2}$	11, 11	$.2853 \times 10^{-2}$
4, 19	$.9989 \times 10^{-3}$	5, 24	$.1618 \times 10^{-2}$	6, 30	$.2399 \times 10^{-2}$	8, 13	$.2223 \times 10^{-2}$	9, 23	$.4001 \times 10^{-2}$	11, 12	$.3209 \times 10^{-2}$
4, 20	$.1032 \times 10^{-2}$	5, 25	$.1665 \times 10^{-2}$			8, 14	$.2376 \times 10^{-2}$	9, 24	$.4134 \times 10^{-2}$	11, 13	$.3564 \times 10^{-2}$
4, 21	$.1065 \times 10^{-2}$	5, 26	$.1703 \times 10^{-2}$	7, 7	$.8990 \times 10^{-3}$	8, 15	$.2505 \times 10^{-2}$	9, 25	$.4264 \times 10^{-2}$	11, 14	$.3831 \times 10^{-2}$
4, 22	$.1089 \times 10^{-2}$	5, 27	$.1733 \times 10^{-2}$	7, 8	$.1043 \times 10^{-2}$	8, 16	$.2596 \times 10^{-2}$	9, 26	$.4367 \times 10^{-2}$	11, 15	$.4057 \times 10^{-2}$
4, 23	$.1115 \times 10^{-2}$	5, 28	$.1753 \times 10^{-2}$	7, 9	$.1206 \times 10^{-2}$	8, 17	$.2716 \times 10^{-2}$	9, 27	$.4448 \times 10^{-2}$	11, 16	$.4217 \times 10^{-2}$
4, 24	$.1148 \times 10^{-2}$	5, 29	$.1775 \times 10^{-2}$	7, 10	$.1369 \times 10^{-2}$	8, 18	$.2837 \times 10^{-2}$	9, 28	$.4503 \times 10^{-2}$	11, 17	$.4428 \times 10^{-2}$
4, 25	$.1181 \times 10^{-2}$	5, 30	$.1800 \times 10^{-2}$	7, 11	$.1533 \times 10^{-2}$	8, 19	$.2949 \times 10^{-2}$	9, 29	$.4564 \times 10^{-2}$	11, 18	$.4639 \times 10^{-2}$
4, 26	$.1208 \times 10^{-2}$			7, 12	$.1698 \times 10^{-2}$	8, 20	$.3055 \times 10^{-2}$	9, 30	$.4635 \times 10^{-2}$	11, 19	$.4838 \times 10^{-2}$
4, 27	$.1228 \times 10^{-2}$	6, 6	$.5687 \times 10^{-3}$	7, 13	$.1863 \times 10^{-2}$	8, 21	$.3161 \times 10^{-2}$			11, 20	$.5023 \times 10^{-2}$
4, 28	$.1242 \times 10^{-2}$	6, 7	$.7099 \times 10^{-3}$	7, 14	$.1987 \times 10^{-2}$	8, 22	$.3236 \times 10^{-2}$	10, 10	$.2204 \times 10^{-2}$	11, 21	$.5209 \times 10^{-2}$
4, 29	$.1258 \times 10^{-2}$	6, 8	$.8163 \times 10^{-3}$	7, 15	$.2092 \times 10^{-2}$	8, 23	$.3320 \times 10^{-2}$	10, 11	$.2501 \times 10^{-2}$	11, 22	$.5341 \times 10^{-2}$
4, 30	$.1276 \times 10^{-2}$	6, 9	$.9371 \times 10^{-3}$	7, 16	$.2167 \times 10^{-2}$	8, 24	$.3428 \times 10^{-2}$	10, 12	$.2801 \times 10^{-2}$	11, 23	$.5489 \times 10^{-2}$
		6, 10	$.1058 \times 10^{-2}$	7, 17	$.2265 \times 10^{-2}$	8, 25	$.3534 \times 10^{-2}$	10, 13	$.3100 \times 10^{-2}$	11, 24	$.5678 \times 10^{-2}$
5, 5	$.3563 \times 10^{-3}$	6, 11	$.1179 \times 10^{-2}$	7, 18	$.2363 \times 10^{-2}$	8, 26	$.3618 \times 10^{-2}$	10, 14	$.3326 \times 10^{-2}$	11, 25	$.5863 \times 10^{-2}$
5, 6	$.4469 \times 10^{-3}$	6, 12	$.1302 \times 10^{-2}$	7, 19	$.2455 \times 10^{-2}$	8, 27	$.3684 \times 10^{-2}$	10, 15	$.3516 \times 10^{-2}$	11, 26	$.6011 \times 10^{-2}$
5, 7	$.5514 \times 10^{-3}$	6, 13	$.1424 \times 10^{-2}$	7, 20	$.2541 \times 10^{-2}$	8, 28	$.3729 \times 10^{-2}$	10, 16	$.3652 \times 10^{-2}$	11, 27	$.6126 \times 10^{-2}$
5, 8	$.6301 \times 10^{-3}$	6, 14	$.1516 \times 10^{-2}$	7, 21	$.2627 \times 10^{-2}$	8, 29	$.3778 \times 10^{-2}$	10, 17	$.3830 \times 10^{-2}$	11, 28	$.6205 \times 10^{-2}$
5, 9	$.7194 \times 10^{-3}$	6, 15	$.1594 \times 10^{-2}$	7, 22	$.2689 \times 10^{-2}$	8, 30	$.3836 \times 10^{-2}$	10, 18	$.4008 \times 10^{-2}$	11, 29	$.6291 \times 10^{-2}$
5, 10	$.8088 \times 10^{-3}$	6, 16	$.1649 \times 10^{-2}$	7, 23	$.2758 \times 10^{-2}$			10, 19	$.4175 \times 10^{-2}$	11, 30	$.6393 \times 10^{-2}$
5, 11	$.8987 \times 10^{-3}$	6, 17	$.1722 \times 10^{-2}$	7, 24	$.2845 \times 10^{-2}$	9, 9	$.1663 \times 10^{-2}$	10, 20	$.4332 \times 10^{-2}$		
5, 12	$.9892 \times 10^{-3}$	6, 18	$.1795 \times 10^{-2}$	7, 25	$.2931 \times 10^{-2}$	9, 10	$.1909 \times 10^{-2}$	10, 21	$.4488 \times 10^{-2}$	12, 12	$.3623 \times 10^{-2}$
5, 13	$.1080 \times 10^{-2}$	6, 19	$.1863 \times 10^{-2}$	7, 26	$.3000 \times 10^{-2}$	9, 11	$.2156 \times 10^{-2}$	10, 22	$.4600 \times 10^{-2}$	12, 13	$.4039 \times 10^{-2}$
5, 14	$.1148 \times 10^{-2}$	6, 20	$.1927 \times 10^{-2}$	7, 27	$.3054 \times 10^{-2}$	9, 12	$.2404 \times 10^{-2}$	10, 23	$.4724 \times 10^{-2}$	12, 14	$.4352 \times 10^{-2}$
						9, 13	$.2653 \times 10^{-2}$			12, 15	$.4616 \times 10^{-2}$

TABLE V.- INFLUENCE COEFFICIENTS - Concluded

i, j	$\sigma_{i,j}$, in./lb	i, j	$\sigma_{i,j}$, in./lb	i, j	$\sigma_{i,j}$, in./lb	i, j	$\sigma_{i,j}$, in./lb	i, j	$\sigma_{i,j}$, in./lb	i, j	$\sigma_{i,j}$, in./lb
12, 16	0.4804×10^{-2}	13, 29	0.8211×10^{-2}	15, 27	0.9379×10^{-2}	17, 29	0.1090×10^{-1}	20, 24	0.1168×10^{-1}	23, 28	0.1511×10^{-1}
12, 17	$.5051 \times 10^{-2}$	13, 30	$.8348 \times 10^{-2}$	15, 28	$.9508 \times 10^{-2}$	17, 30	$.1109 \times 10^{-1}$	20, 25	$.1216 \times 10^{-1}$	23, 29	$.1540 \times 10^{-1}$
12, 18	$.5298 \times 10^{-2}$			15, 29	$.9649 \times 10^{-2}$			20, 26	$.1255 \times 10^{-1}$	23, 30	$.1574 \times 10^{-1}$
12, 19	$.5530 \times 10^{-2}$	14, 14	$.5283 \times 10^{-2}$	15, 30	$.9815 \times 10^{-2}$	18, 18	$.8164 \times 10^{-2}$	20, 27	$.1285 \times 10^{-1}$		
12, 20	$.5748 \times 10^{-2}$	14, 15	$.5621 \times 10^{-2}$			18, 19	$.8588 \times 10^{-2}$	20, 28	$.1305 \times 10^{-1}$	24, 24	$.1407 \times 10^{-1}$
12, 21	$.5965 \times 10^{-2}$	14, 16	$.5862 \times 10^{-2}$	16, 16	$.6533 \times 10^{-2}$	18, 20	$.8985 \times 10^{-2}$	20, 29	$.1328 \times 10^{-1}$	24, 25	$.1478 \times 10^{-1}$
12, 22	$.6119 \times 10^{-2}$	14, 17	$.6178 \times 10^{-2}$	16, 17	$.6902 \times 10^{-2}$	18, 21	$.9382 \times 10^{-2}$	20, 30	$.1354 \times 10^{-1}$	24, 26	$.1535 \times 10^{-1}$
12, 23	$.6292 \times 10^{-2}$	14, 18	$.6495 \times 10^{-2}$	16, 18,	$.7272 \times 10^{-2}$	18, 22	$.9664 \times 10^{-2}$			24, 27	$.1579 \times 10^{-1}$
12, 24	$.6513 \times 10^{-2}$	14, 19	$.6792 \times 10^{-2}$	16, 19	$.7618 \times 10^{-2}$	18, 23	$.9979 \times 10^{-2}$	21, 21	$.1099 \times 10^{-1}$	24, 28	$.1609 \times 10^{-1}$
12, 25	$.6730 \times 10^{-2}$	14, 20	$.7071 \times 10^{-2}$	16, 20	$.7944 \times 10^{-2}$	18, 24	$.1038 \times 10^{-1}$	21, 22	$.1137 \times 10^{-1}$	24, 29	$.1643 \times 10^{-1}$
12, 26	$.6903 \times 10^{-2}$	14, 21	$.7350 \times 10^{-2}$	16, 21	$.8269 \times 10^{-2}$	18, 25	$.1078 \times 10^{-1}$	21, 23	$.1179 \times 10^{-1}$	24, 30	$.1681 \times 10^{-1}$
12, 27	$.7038 \times 10^{-2}$	14, 22	$.7548 \times 10^{-2}$	16, 22	$.8500 \times 10^{-2}$	18, 26	$.1109 \times 10^{-1}$	21, 24	$.1234 \times 10^{-1}$		
12, 28	$.7130 \times 10^{-2}$	14, 23	$.7769 \times 10^{-2}$	16, 23	$.8758 \times 10^{-2}$	18, 27	$.1134 \times 10^{-1}$	21, 25	$.1287 \times 10^{-1}$	25, 25	$.1561 \times 10^{-1}$
12, 29	$.7231 \times 10^{-2}$	14, 24	$.8053 \times 10^{-2}$	16, 24	$.9089 \times 10^{-2}$	18, 28	$.1151 \times 10^{-1}$	21, 26	$.1329 \times 10^{-1}$	25, 26	$.1628 \times 10^{-1}$
12, 30	$.7350 \times 10^{-2}$	14, 25	$.8331 \times 10^{-2}$	16, 25	$.9413 \times 10^{-2}$	18, 29	$.1169 \times 10^{-1}$	21, 27	$.1362 \times 10^{-1}$	25, 27	$.1680 \times 10^{-1}$
		14, 26	$.8552 \times 10^{-2}$	16, 26	$.9672 \times 10^{-2}$	18, 30	$.1191 \times 10^{-1}$	21, 28	$.1385 \times 10^{-1}$	25, 28	$.1716 \times 10^{-1}$
13, 13	$.4519 \times 10^{-2}$	14, 27	$.8726 \times 10^{-2}$	16, 27	$.9874 \times 10^{-2}$			21, 29	$.1410 \times 10^{-1}$	25, 29	$.1755 \times 10^{-1}$
13, 14	$.4881 \times 10^{-2}$	14, 28	$.8844 \times 10^{-2}$	16, 28	$.1001 \times 10^{-1}$	19, 19	$.9055 \times 10^{-2}$	21, 30	$.1439 \times 10^{-1}$	25, 30	$.1801 \times 10^{-1}$
13, 15	$.5187 \times 10^{-2}$	14, 29	$.8973 \times 10^{-2}$	16, 29	$.1016 \times 10^{-1}$	19, 20	$.9494 \times 10^{-2}$				
13, 16	$.5404 \times 10^{-2}$	14, 30	$.9126 \times 10^{-2}$	16, 30	$.1034 \times 10^{-1}$	19, 21	$.9933 \times 10^{-2}$	22, 22	$.1178 \times 10^{-1}$	26, 26	$.1706 \times 10^{-1}$
13, 17	$.5689 \times 10^{-2}$					19, 22	$.1025 \times 10^{-1}$	22, 23	$.1223 \times 10^{-1}$	26, 27	$.1769 \times 10^{-1}$
13, 18	$.5975 \times 10^{-2}$	15, 15	$.5990 \times 10^{-2}$	17, 17	$.7308 \times 10^{-2}$	19, 23	$.1059 \times 10^{-1}$	22, 24	$.1281 \times 10^{-1}$	26, 28	$.1812 \times 10^{-1}$
13, 19	$.6243 \times 10^{-2}$	15, 16	$.6253 \times 10^{-2}$	17, 18	$.7714 \times 10^{-2}$	19, 24	$.1104 \times 10^{-1}$	22, 25	$.1338 \times 10^{-1}$	26, 29	$.1859 \times 10^{-1}$
13, 20	$.6495 \times 10^{-2}$	15, 17	$.6598 \times 10^{-2}$	17, 19	$.8096 \times 10^{-2}$	19, 25	$.1148 \times 10^{-1}$	22, 26	$.1383 \times 10^{-1}$	26, 30	$.1915 \times 10^{-1}$
13, 21	$.6746 \times 10^{-2}$	15, 18	$.6944 \times 10^{-2}$	17, 20	$.8454 \times 10^{-2}$	19, 26	$.1183 \times 10^{-1}$	22, 27	$.1419 \times 10^{-1}$		
13, 22	$.6925 \times 10^{-2}$	15, 19	$.7268 \times 10^{-2}$	17, 21	$.8812 \times 10^{-2}$	19, 27	$.1210 \times 10^{-1}$	22, 28	$.1443 \times 10^{-1}$	27, 27	$.1847 \times 10^{-1}$
13, 23	$.7124 \times 10^{-2}$	15, 20	$.7573 \times 10^{-2}$	17, 22	$.9067 \times 10^{-2}$	19, 28	$.1229 \times 10^{-1}$	22, 29	$.1469 \times 10^{-1}$	27, 28	$.1899 \times 10^{-1}$
13, 24	$.7380 \times 10^{-2}$	15, 21	$.7877 \times 10^{-2}$	17, 23	$.9351 \times 10^{-2}$	19, 29	$.1249 \times 10^{-1}$	22, 30	$.1501 \times 10^{-1}$	27, 29	$.1957 \times 10^{-1}$
13, 25	$.7631 \times 10^{-2}$	15, 22	$.8093 \times 10^{-2}$	17, 24	$.9716 \times 10^{-2}$	19, 30	$.1273 \times 10^{-1}$			27, 30	$.2025 \times 10^{-1}$
13, 26	$.7831 \times 10^{-2}$	15, 23	$.8335 \times 10^{-2}$	17, 25	$.1007 \times 10^{-1}$			23, 23	$.1272 \times 10^{-1}$		
13, 27	$.7987 \times 10^{-2}$	15, 24	$.8645 \times 10^{-2}$	17, 26	$.1036 \times 10^{-1}$	20, 20	$.9977 \times 10^{-2}$	23, 24	$.1335 \times 10^{-1}$	28, 28	$.1959 \times 10^{-1}$
13, 28	$.8094 \times 10^{-2}$	15, 25	$.8948 \times 10^{-2}$	17, 27	$.1058 \times 10^{-1}$	20, 21	$.1046 \times 10^{-1}$	23, 25	$.1397 \times 10^{-1}$	28, 29	$.2025 \times 10^{-1}$
		15, 26	$.9190 \times 10^{-2}$	17, 28	$.1073 \times 10^{-1}$	20, 22	$.1080 \times 10^{-1}$	23, 26	$.1446 \times 10^{-1}$	28, 30	$.2102 \times 10^{-1}$
						20, 23	$.1119 \times 10^{-1}$	23, 27	$.1485 \times 10^{-1}$		
										29, 29	$.2100 \times 10^{-1}$
										29, 30	$.2188 \times 10^{-1}$
										30, 30	$.2294 \times 10^{-1}$

TABLE VI.- EXPERIMENTALLY DETERMINED

DAMPING COEFFICIENTS

Test	Mode	Average damping coefficient*
2	1	0.035
2	2	0.054
2	3	0.050
3	1	0.042
3	2	0.049
3	3	0.069

*The complex damping coefficient is defined as twice the ratio of the equivalent viscous damping coefficient to the critical damping.

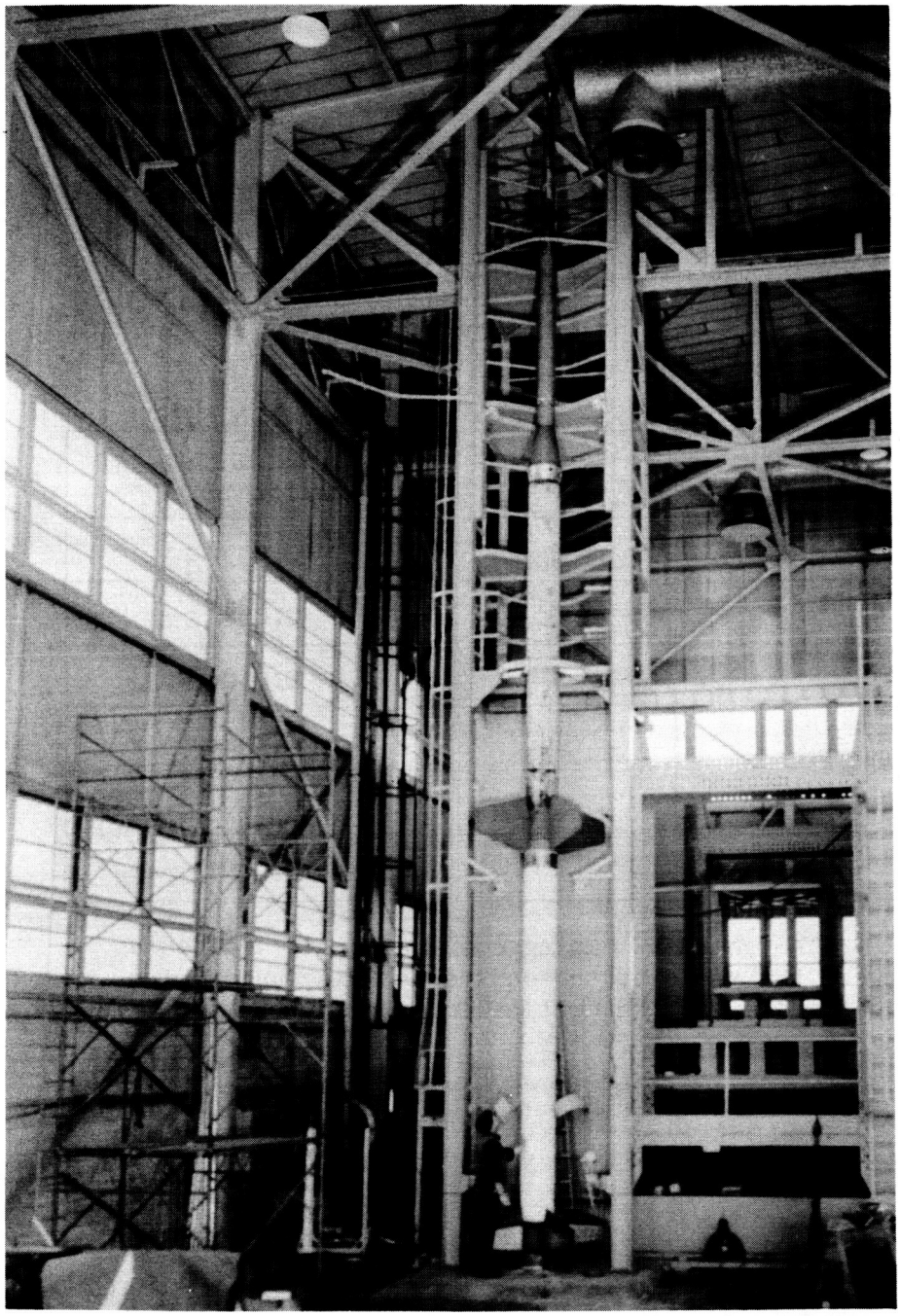

L-61-437

Figure 1.- Photograph of assembled vehicle and test stand.

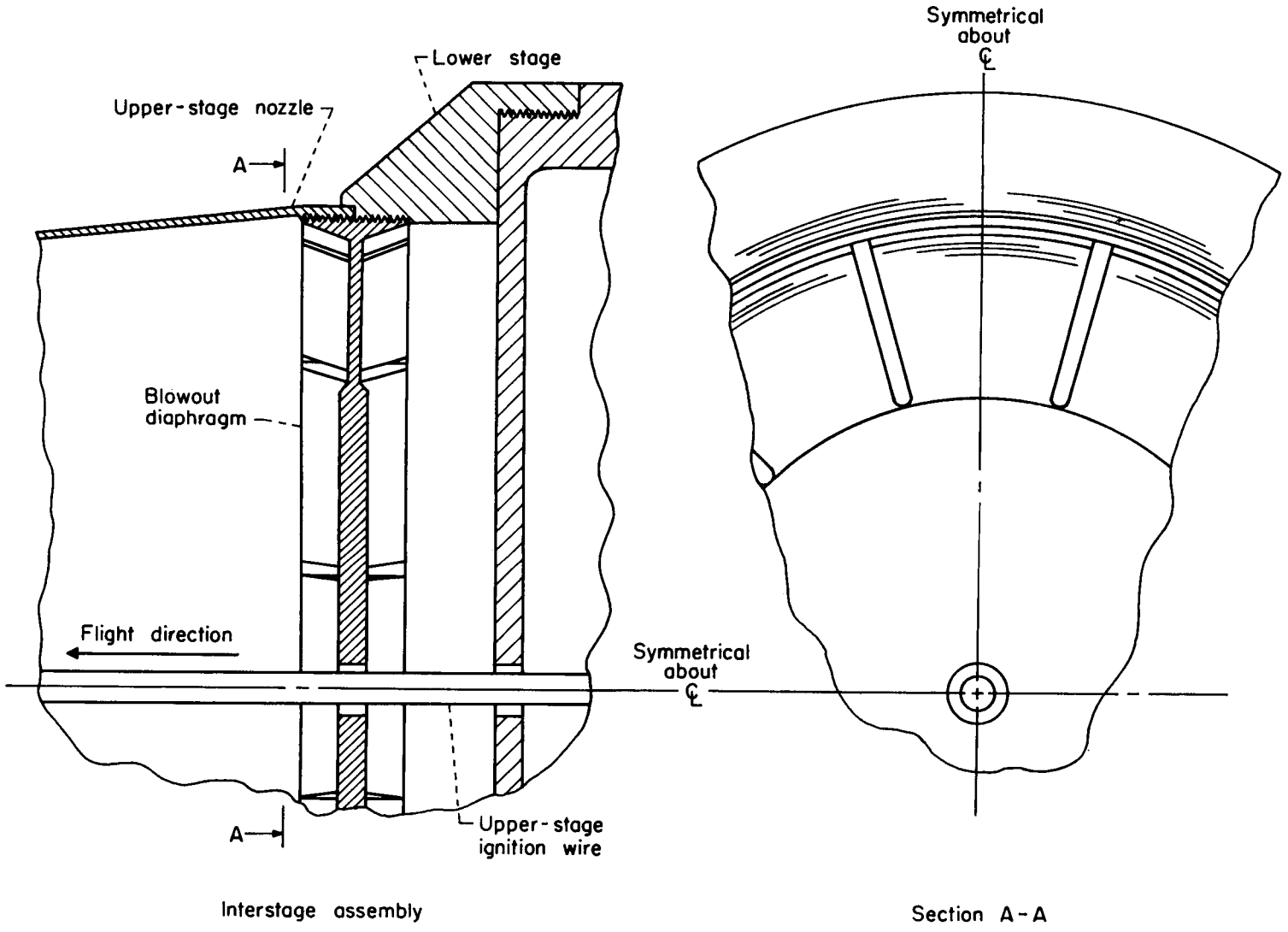

Figure 2.- Diagram of typical blowout diaphragm installation.

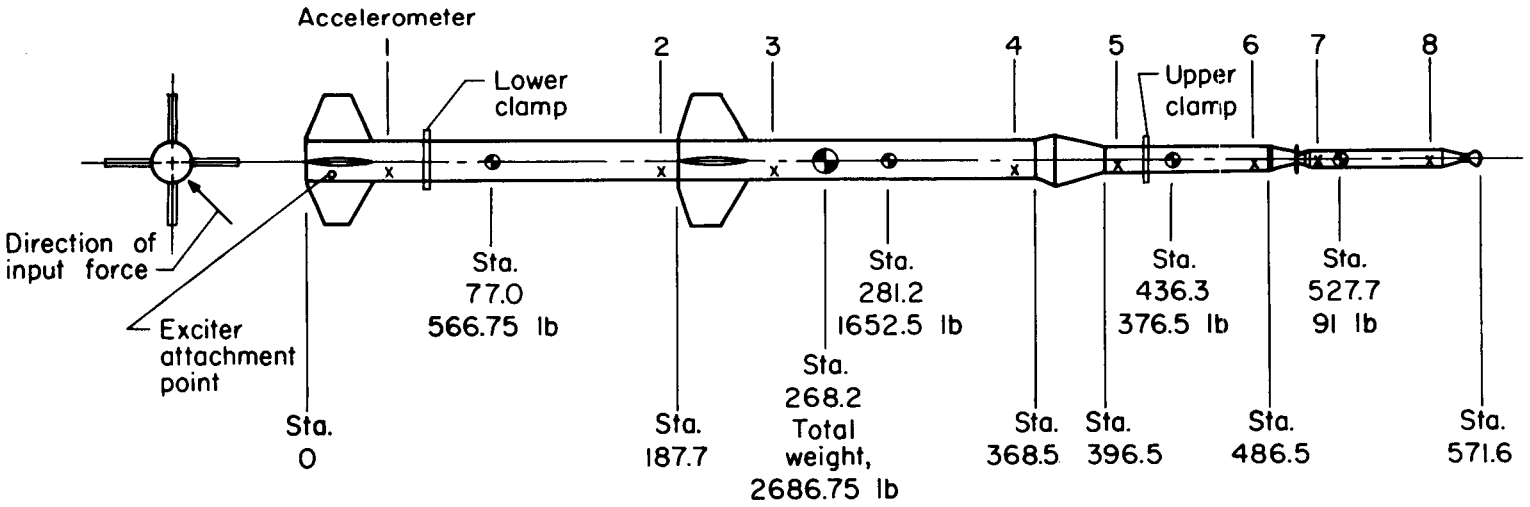

Test	Lower-clamp station	Station of accelerometer							
		1	2	3	4	5	6	7	8
1	74.43	31.5	170.41	222.11	356.04	402.57	478.35	512.85	539.41
2	150.91	31.5	170.41	222.11	356.04	402.57	478.35	512.85	539.41
3	150.91	33.65	170.90	220.24	355.42	401.40	476.35	513.35	540.22

Figure 3.- Schematic diagram of vehicle. Stations are given in inches.

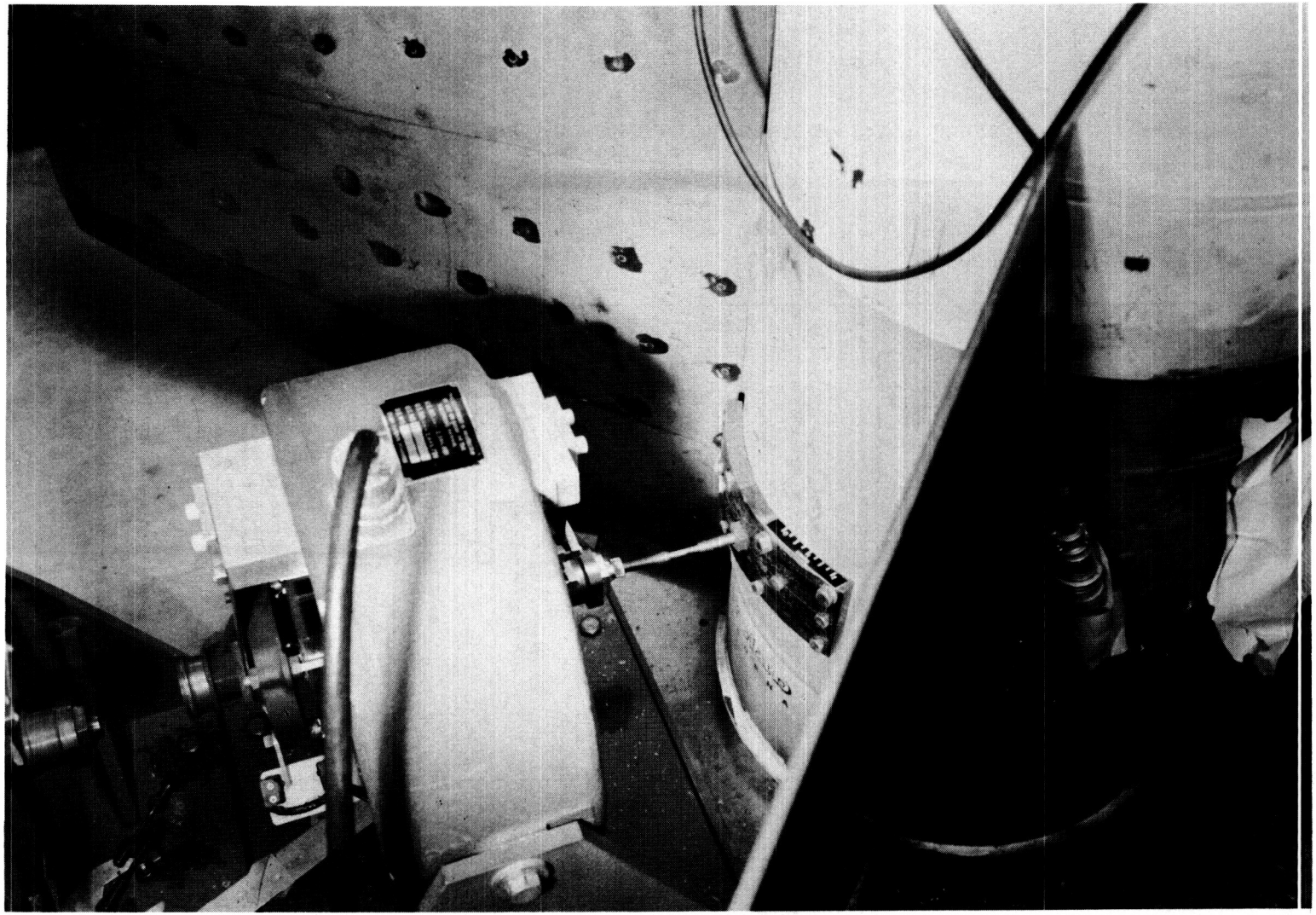

Figure 4.- Photograph of exciter attached to vehicle. L-61-1159

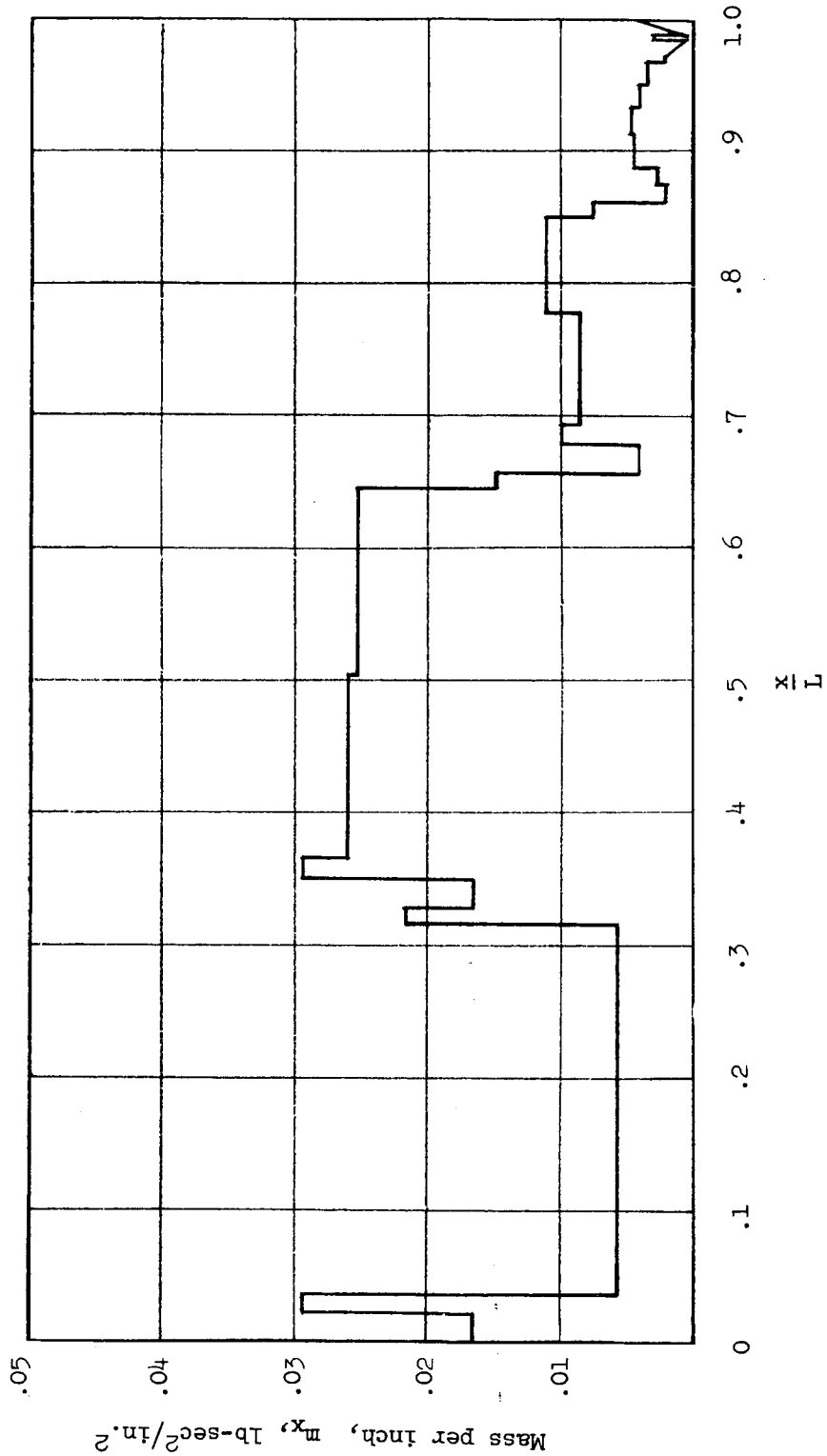

Figure 5.- Mass per inch at burnout of first stage.

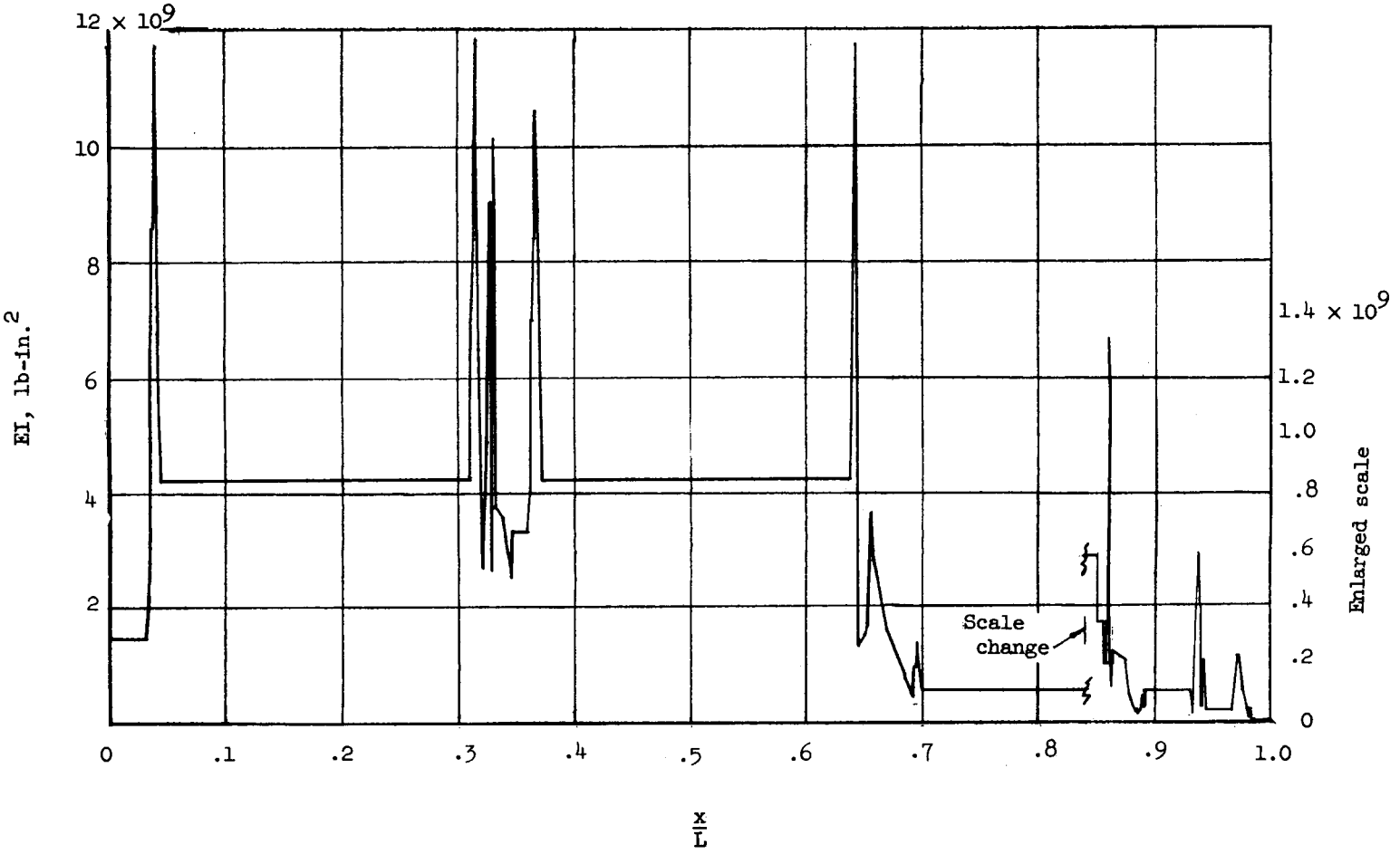

Figure 6.- Stiffness coefficient.

Excellent joint:
Butt welded skin
Heavy bolted, preloaded

Good joint:
Heavy flange bolted
Threaded on sleeve with preloaded shoulder
Threaded diaphragm with butt
Marman bands

Moderate joint:
Riveted, lapped
Riveted to inner ring
Screw section without butt

Loose joint:
Light flanges, bolted or riveted
Lapped with screw fasteners
Equally spaced brackets

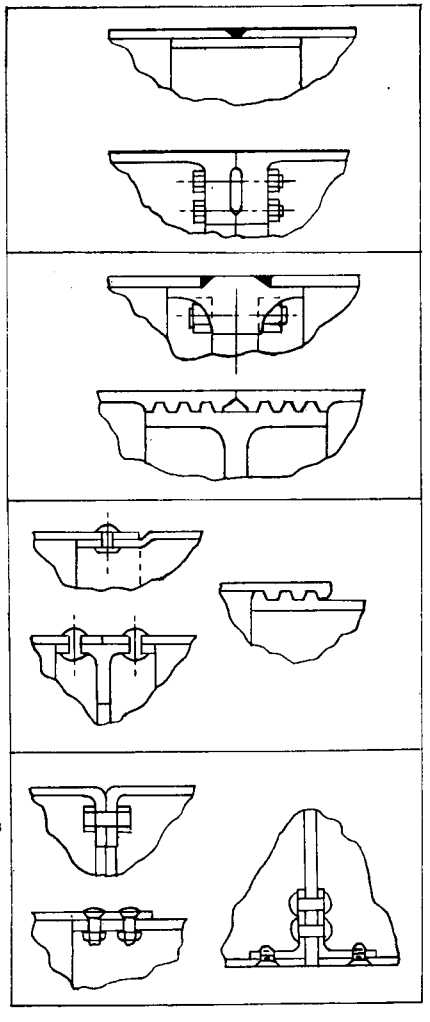

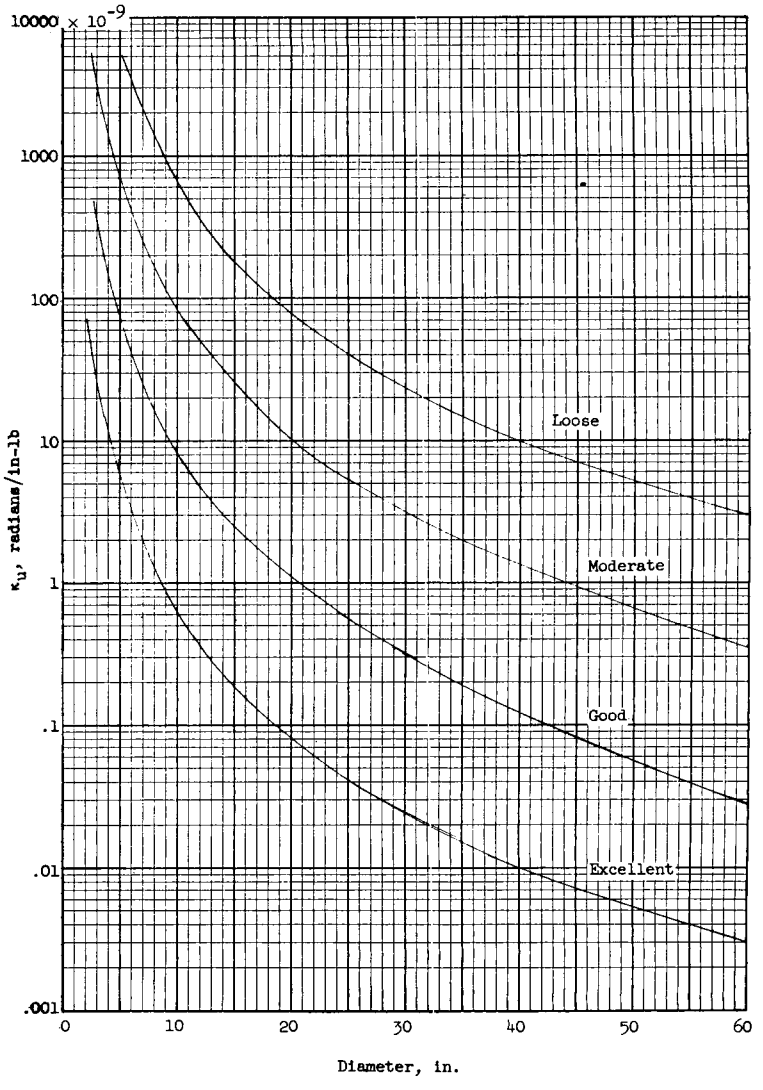

Figure 7.- Joint rotation constants.

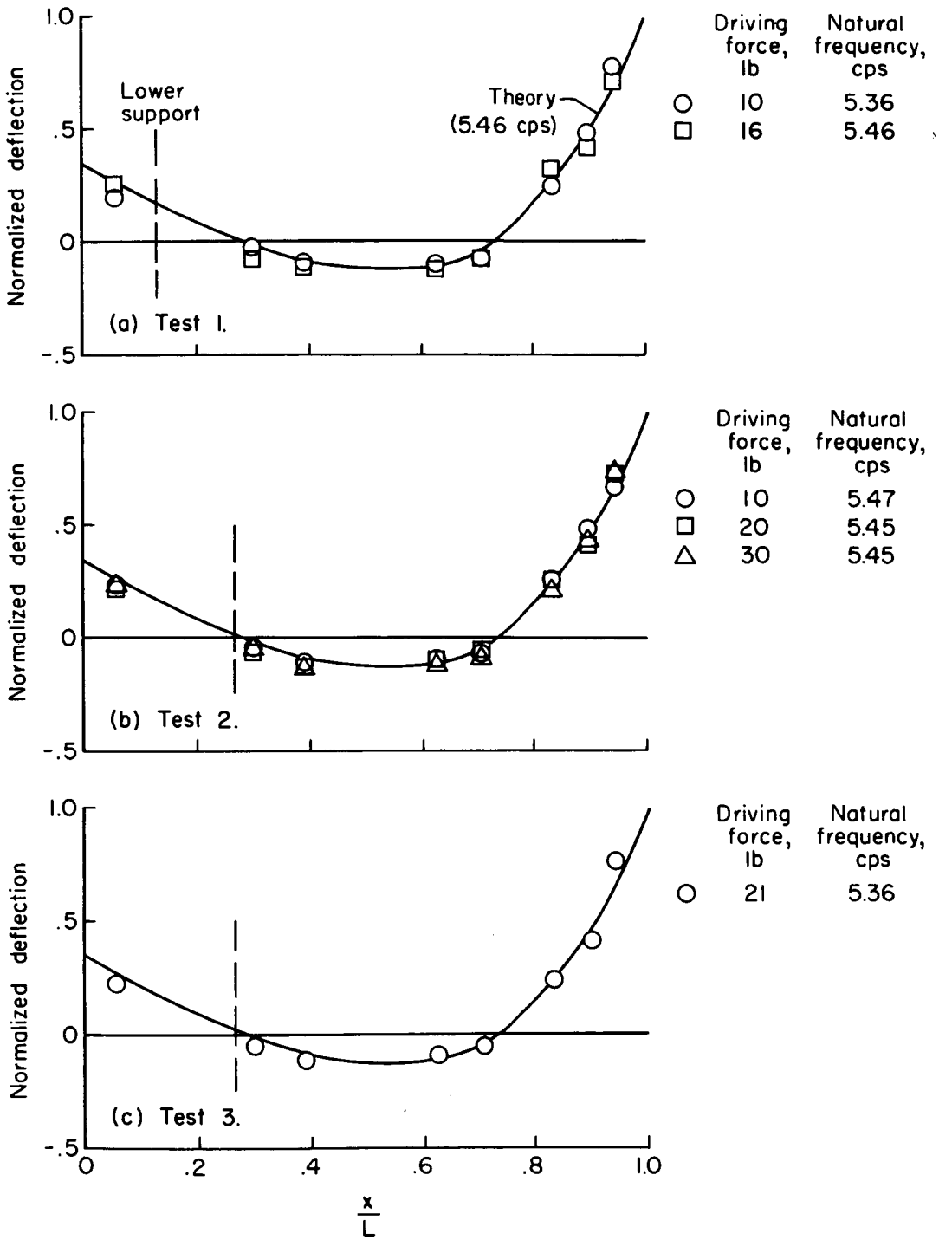

Figure 8.- Comparison of the experimental and theoretical natural frequencies and mode shapes for the first free-free mode.

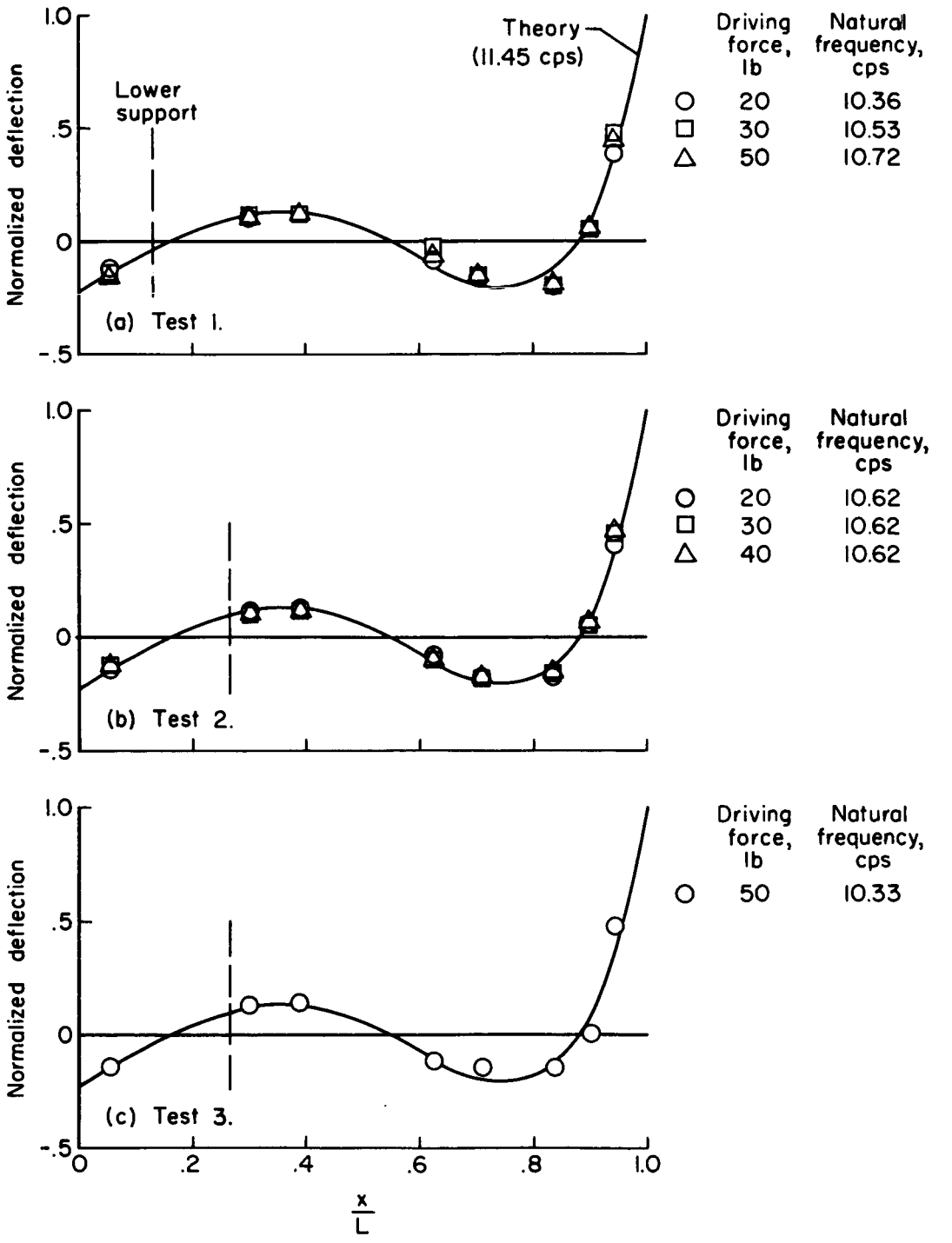

Figure 9.- Comparison of the experimental and theoretical natural frequencies and mode shapes for the second free-free mode.

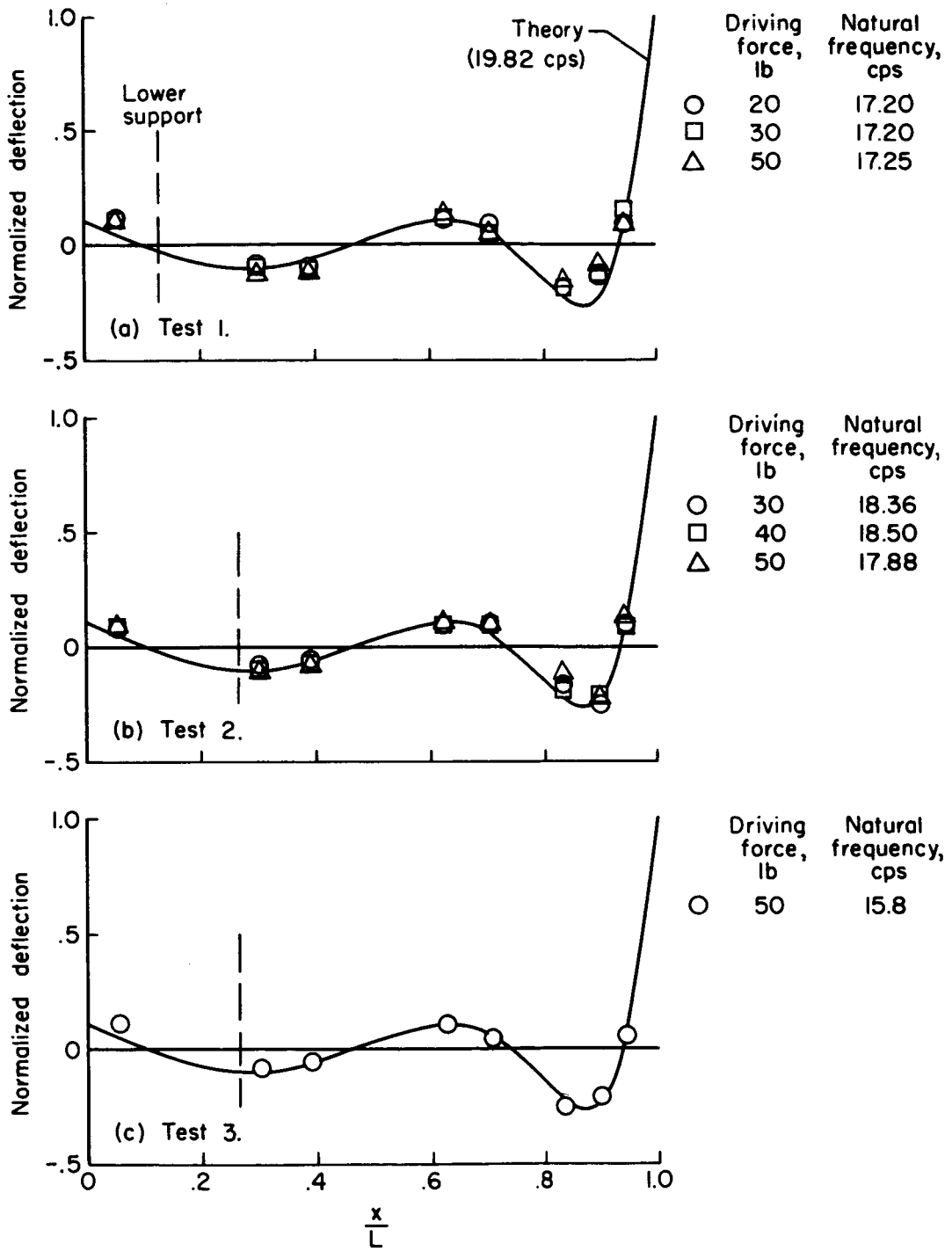

Figure 10.- Comparison of the experimental and theoretical natural frequencies and mode shapes for the third free-free mode.

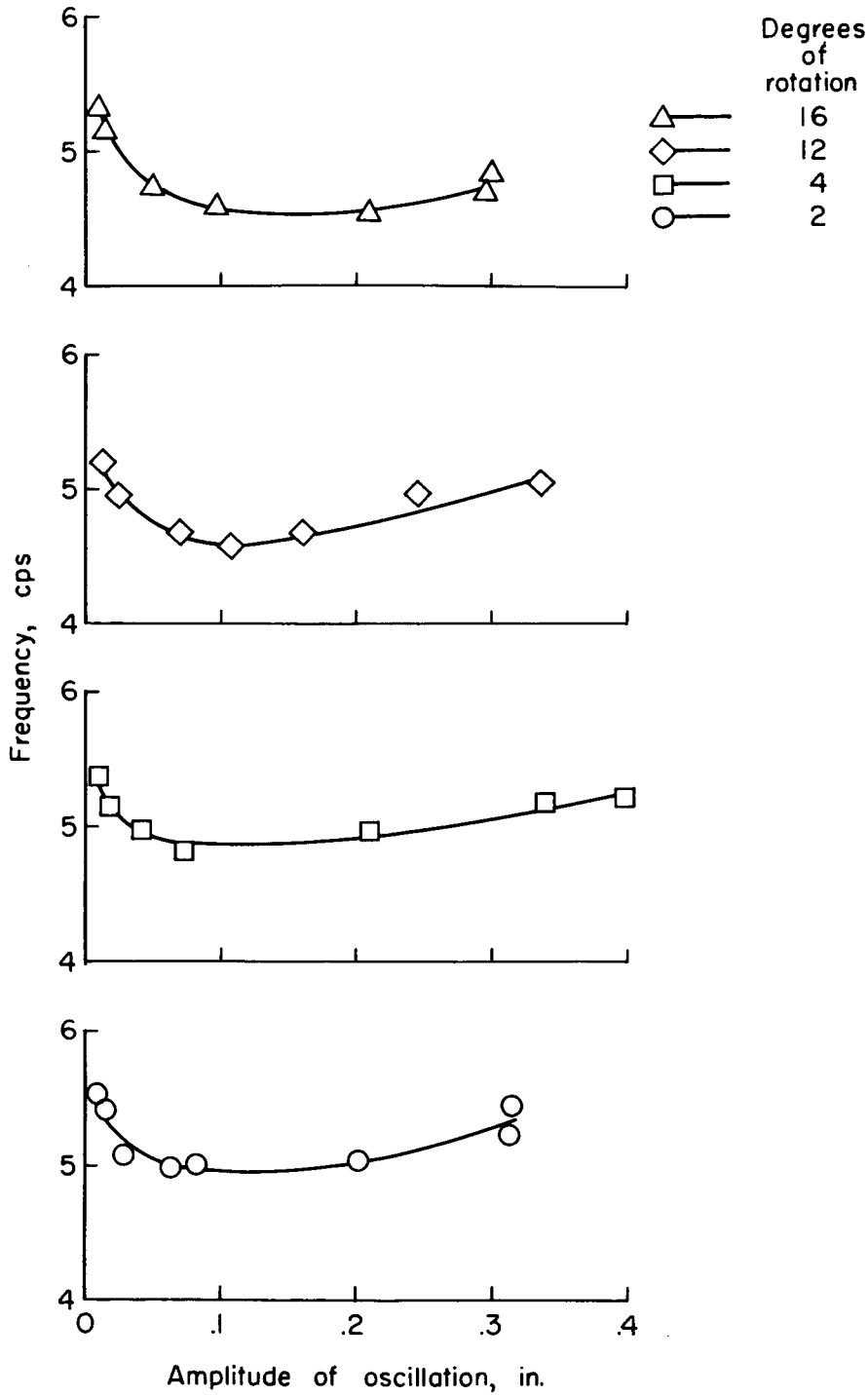

Figure 11.- Variation of frequency with amplitude for different amounts of rotation of joint between first and second stages.

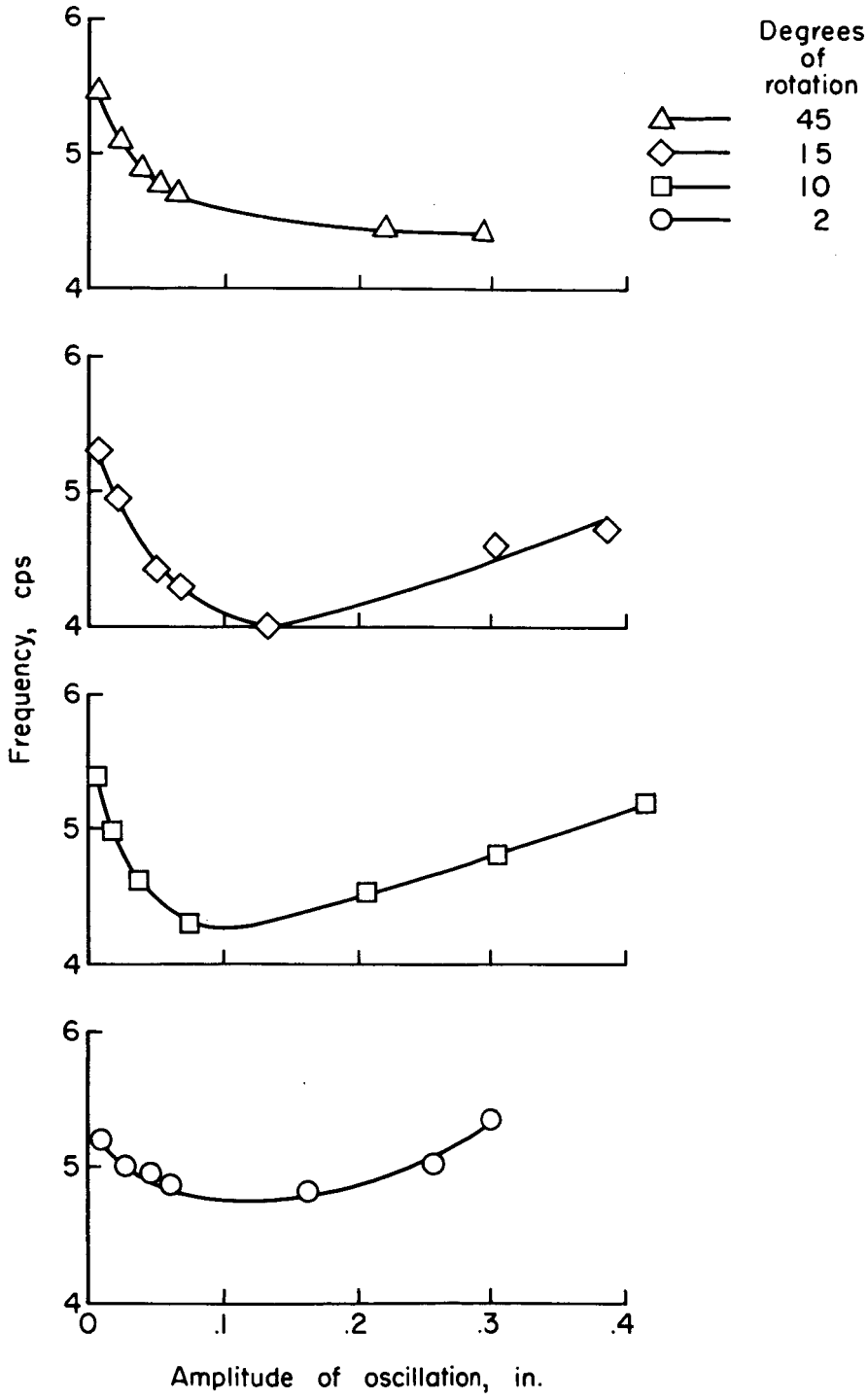

Figure 12.- Variation of frequency with amplitude for different amounts of rotation of joint between second and third stages.

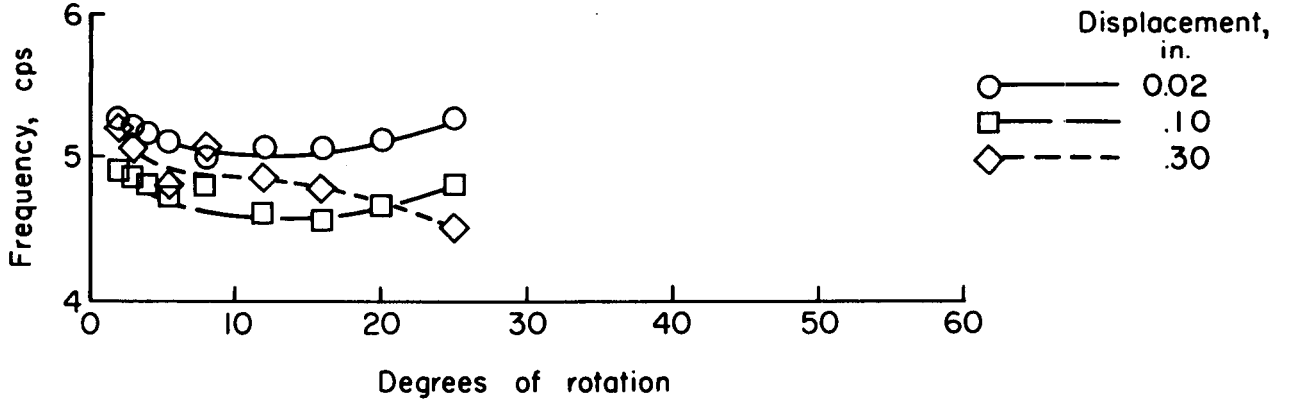

(a) Rotation of joint between first and second stages.

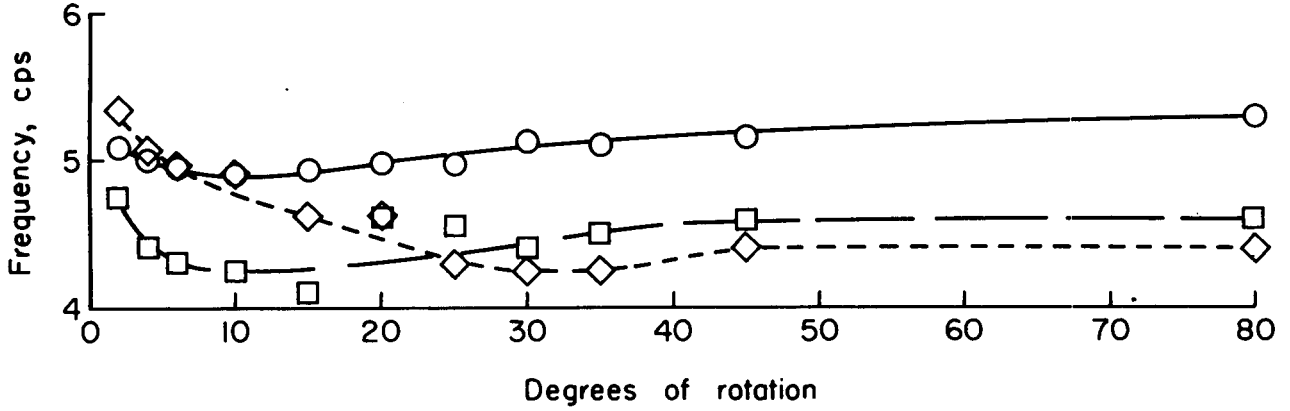

(b) Rotation of joint between second and third stages.

Figure 13.- Variation of frequency with degrees of rotation or unwinding for different amplitudes of oscillation.

NASA-Langley, 1962 L-1669

N62-14464

ERRATA

NASA Technical Note D-1354

AN EXPERIMENTAL AND ANALYTICAL INVESTIGATION OF THE NATURAL FREQUENCIES AND MODE SHAPES OF A FOUR-STAGE SOLID-PROPELLANT ROCKET VEHICLE

By Sumner A. Leadbetter, Vernon L. Alley, Jr.,
Robert W. Herr, and A. Harper Gerringer

August 1962

Page 10, fifth line from bottom: 0.01755 in./lb should be 0.01495 in./lb

Page 10, third line from bottom: $\alpha_{25,29} = 0.01721$ should be $\alpha_{25,29} = 0.01461$

Page 11, line 9: 2.0 percent should be 2.3 percent

Page 11, line 10: 6.7-percent increase should be 7.0-percent increase

Table IV, page 25: In the column headed "Joint location, x/L," the value .9376 should be .9370

Table V, pages 26 to 28: Replace entire table. The changes have no effect on other modal data.

NASA-Langley, 1968

Issued 11-25-68

TABLE V.- INFLUENCE COEFFICIENTS

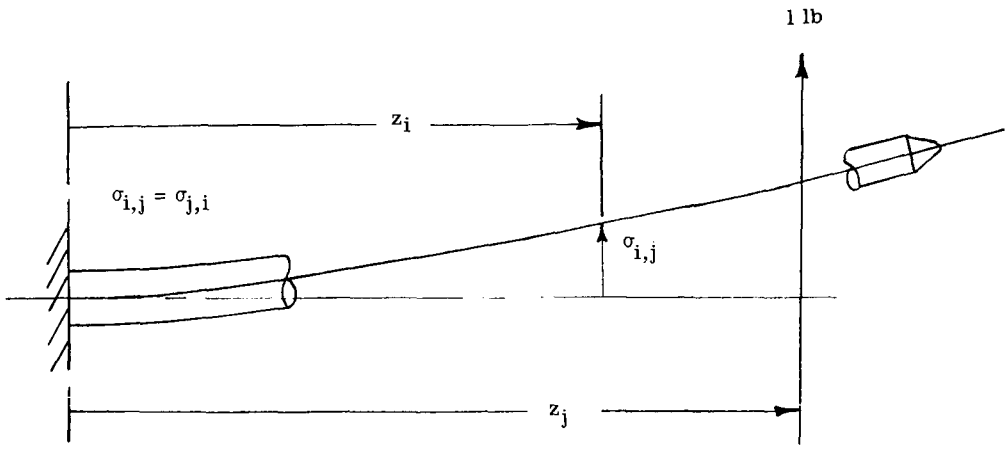

i,j	$\sigma_{i,j}$, in./lb	i,j	$\sigma_{i,j}$, in./lb	i,j	$\sigma_{i,j}$, in./lb	i,j	$\sigma_{i,j}$, in./lb
1, 1	0.1475×10^{-5}	2, 2	0.1269×10^{-4}	3, 3	0.4249×10^{-4}	4, 4	0.1000×10^{-3}
1, 2	$.3888 \times 10^{-5}$	2, 3	$.2221 \times 10^{-4}$	3, 4	$.6360 \times 10^{-4}$	4, 5	$.1374 \times 10^{-3}$
1, 3	$.6302 \times 10^{-5}$	2, 4	$.3177 \times 10^{-4}$	3, 5	$.8484 \times 10^{-4}$	4, 6	$.1749 \times 10^{-3}$
1, 4	$.8729 \times 10^{-5}$	2, 5	$.4140 \times 10^{-4}$	3, 6	$.1061 \times 10^{-3}$	4, 7	$.2181 \times 10^{-3}$
1, 5	$.1117 \times 10^{-4}$	2, 6	$.5105 \times 10^{-4}$	3, 7	$.1306 \times 10^{-3}$	4, 8	$.2506 \times 10^{-3}$
1, 6	$.1362 \times 10^{-4}$	2, 7	$.6216 \times 10^{-4}$	3, 8	$.1491 \times 10^{-3}$	4, 9	$.2875 \times 10^{-3}$
1, 7	$.1644 \times 10^{-4}$	2, 8	$.7054 \times 10^{-4}$	3, 9	$.1701 \times 10^{-3}$	4, 10	$.3244 \times 10^{-3}$
1, 8	$.1856 \times 10^{-4}$	2, 9	$.8005 \times 10^{-4}$	3, 10	$.1911 \times 10^{-3}$	4, 11	$.3616 \times 10^{-3}$
1, 9	$.2098 \times 10^{-4}$	2, 10	$.8955 \times 10^{-4}$	3, 11	$.2122 \times 10^{-3}$	4, 12	$.3990 \times 10^{-3}$
1, 10	$.2339 \times 10^{-4}$	2, 11	$.9912 \times 10^{-4}$	3, 12	$.2334 \times 10^{-3}$	4, 13	$.4364 \times 10^{-3}$
1, 11	$.2581 \times 10^{-4}$	2, 12	$.1088 \times 10^{-3}$	3, 13	$.2547 \times 10^{-3}$	4, 14	$.4646 \times 10^{-3}$
1, 12	$.2826 \times 10^{-4}$	2, 13	$.1184 \times 10^{-3}$	3, 14	$.2707 \times 10^{-3}$	4, 15	$.4883 \times 10^{-3}$
1, 13	$.3070 \times 10^{-4}$	2, 14	$.1256 \times 10^{-3}$	3, 15	$.2842 \times 10^{-3}$	4, 16	$.5052 \times 10^{-3}$
1, 14	$.3254 \times 10^{-4}$	2, 15	$.1318 \times 10^{-3}$	3, 16	$.2938 \times 10^{-3}$	4, 17	$.5274 \times 10^{-3}$
1, 15	$.3409 \times 10^{-4}$	2, 16	$.1361 \times 10^{-3}$	3, 17	$.3064 \times 10^{-3}$	4, 18	$.5497 \times 10^{-3}$
1, 16	$.3520 \times 10^{-4}$	2, 17	$.1418 \times 10^{-3}$	3, 18	$.3190 \times 10^{-3}$	4, 19	$.5705 \times 10^{-3}$
1, 17	$.3665 \times 10^{-4}$	2, 18	$.1475 \times 10^{-3}$	3, 19	$.3309 \times 10^{-3}$	4, 20	$.5901 \times 10^{-3}$
1, 18	$.3810 \times 10^{-4}$	2, 19	$.1529 \times 10^{-3}$	3, 20	$.3420 \times 10^{-3}$	4, 21	$.6096 \times 10^{-3}$
1, 19	$.3946 \times 10^{-4}$	2, 20	$.1580 \times 10^{-3}$	3, 21	$.3531 \times 10^{-3}$	4, 22	$.6236 \times 10^{-3}$
1, 20	$.4074 \times 10^{-4}$	2, 21	$.1630 \times 10^{-3}$	3, 22	$.3610 \times 10^{-3}$	4, 23	$.6391 \times 10^{-3}$
1, 21	$.4202 \times 10^{-4}$	2, 22	$.1666 \times 10^{-3}$	3, 23	$.3699 \times 10^{-3}$	4, 24	$.6590 \times 10^{-3}$
1, 22	$.4293 \times 10^{-4}$	2, 23	$.1706 \times 10^{-3}$	3, 24	$.3812 \times 10^{-3}$	4, 25	$.6785 \times 10^{-3}$
1, 23	$.4394 \times 10^{-4}$	2, 24	$.1757 \times 10^{-3}$	3, 25	$.3923 \times 10^{-3}$	4, 26	$.6941 \times 10^{-3}$
1, 24	$.4524 \times 10^{-4}$	2, 25	$.1807 \times 10^{-3}$	3, 26	$.4011 \times 10^{-3}$	4, 27	$.7062 \times 10^{-3}$
1, 25	$.4652 \times 10^{-4}$	2, 26	$.1847 \times 10^{-3}$	3, 27	$.4080 \times 10^{-3}$	4, 28	$.7145 \times 10^{-3}$
1, 26	$.4753 \times 10^{-4}$	2, 27	$.1879 \times 10^{-3}$	3, 28	$.4127 \times 10^{-3}$	4, 29	$.7236 \times 10^{-3}$
1, 27	$.4833 \times 10^{-4}$	2, 28	$.1900 \times 10^{-3}$	3, 29	$.4179 \times 10^{-3}$	4, 30	$.7343 \times 10^{-3}$
1, 28	$.4887 \times 10^{-4}$	2, 29	$.1923 \times 10^{-3}$	3, 30	$.4239 \times 10^{-3}$		
1, 29	$.4946 \times 10^{-4}$	2, 30	$.1951 \times 10^{-3}$				
1, 30	$.5016 \times 10^{-4}$						

TABLE V.- INFLUENCE COEFFICIENTS – Continued

i,j	$\sigma_{i,j}$, in./lb	i,j	$\sigma_{i,j}$, in./lb	i,j	$\sigma_{i,j}$, in./lb	i,j	$\sigma_{i,j}$, in./lb
5, 5	0.1948×10^{-3}	6, 26	0.1496×10^{-2}	8, 24	0.2445×10^{-2}	10, 26	0.3879×10^{-2}
5, 6	$.2531 \times 10^{-3}$	6, 27	$.1523 \times 10^{-2}$	8, 25	$.2524 \times 10^{-2}$	10, 27	$.3955 \times 10^{-2}$
5, 7	$.3203 \times 10^{-3}$	6, 28	$.1542 \times 10^{-2}$	8, 26	$.2586 \times 10^{-2}$	10, 28	$.4007 \times 10^{-2}$
5, 8	$.3709 \times 10^{-3}$	6, 29	$.1562 \times 10^{-2}$	8, 27	$.2635 \times 10^{-2}$	10, 29	$.4064 \times 10^{-2}$
5, 9	$.4283 \times 10^{-3}$	6, 30	$.1586 \times 10^{-2}$	8, 28	$.2668 \times 10^{-2}$	10, 30	$.4131 \times 10^{-2}$
5, 10	$.4858 \times 10^{-3}$			8, 29	$.2705 \times 10^{-2}$		
5, 11	$.5436 \times 10^{-3}$	7, 7	0.5682×10^{-3}	8, 30	$.2748 \times 10^{-2}$	11, 11	0.2072×10^{-2}
5, 12	$.6017 \times 10^{-3}$	7, 8	$.6715 \times 10^{-3}$			11, 12	$.2356 \times 10^{-2}$
5, 13	$.6599 \times 10^{-3}$	7, 9	$.7888 \times 10^{-3}$	9, 9	0.1138×10^{-2}	11, 13	$.2640 \times 10^{-2}$
5, 14	$.7038 \times 10^{-3}$	7, 10	$.9061 \times 10^{-3}$	9, 10	$.1326 \times 10^{-2}$	11, 14	$.2854 \times 10^{-2}$
5, 15	$.7407 \times 10^{-3}$	7, 11	$.1024 \times 10^{-2}$	9, 11	$.1515 \times 10^{-2}$	11, 15	$.3035 \times 10^{-2}$
5, 16	$.7670 \times 10^{-3}$	7, 12	$.1143 \times 10^{-2}$	9, 12	$.1706 \times 10^{-2}$	11, 16	$.3163 \times 10^{-2}$
5, 17	$.8016 \times 10^{-3}$	7, 13	$.1262 \times 10^{-2}$	9, 13	$.1896 \times 10^{-2}$	11, 17	$.3332 \times 10^{-2}$
5, 18	$.8361 \times 10^{-3}$	7, 14	$.1351 \times 10^{-2}$	9, 14	$.2040 \times 10^{-2}$	11, 18	$.3500 \times 10^{-2}$
5, 19	$.8686 \times 10^{-3}$	7, 15	$.1427 \times 10^{-2}$	9, 15	$.2161 \times 10^{-2}$	11, 19	$.3659 \times 10^{-2}$
5, 20	$.8990 \times 10^{-3}$	7, 16	$.1480 \times 10^{-2}$	9, 16	$.2247 \times 10^{-2}$	11, 20	$.3807 \times 10^{-2}$
5, 21	$.9294 \times 10^{-3}$	7, 17	$.1551 \times 10^{-2}$	9, 17	$.2360 \times 10^{-2}$	11, 21	$.3956 \times 10^{-2}$
5, 22	$.9511 \times 10^{-3}$	7, 18	$.1622 \times 10^{-2}$	9, 18	$.2473 \times 10^{-2}$	11, 22	$.4062 \times 10^{-2}$
5, 23	$.9753 \times 10^{-3}$	7, 19	$.1688 \times 10^{-2}$	9, 19	$.2579 \times 10^{-2}$	11, 23	$.4180 \times 10^{-2}$
5, 24	$.1006 \times 10^{-2}$	7, 20	$.1750 \times 10^{-2}$	9, 20	$.2679 \times 10^{-2}$	11, 24	$.4331 \times 10^{-2}$
5, 25	$.1037 \times 10^{-2}$	7, 21	$.1812 \times 10^{-2}$	9, 21	$.2778 \times 10^{-2}$	11, 25	$.4479 \times 10^{-2}$
5, 26	$.1061 \times 10^{-2}$	7, 22	$.1856 \times 10^{-2}$	9, 22	$.2849 \times 10^{-2}$	11, 26	$.4597 \times 10^{-2}$
5, 27	$.1080 \times 10^{-2}$	7, 23	$.1906 \times 10^{-2}$	9, 23	$.2928 \times 10^{-2}$	11, 27	$.4690 \times 10^{-2}$
5, 28	$.1093 \times 10^{-2}$	7, 24	$.1969 \times 10^{-2}$	9, 24	$.3030 \times 10^{-2}$	11, 28	$.4752 \times 10^{-2}$
5, 29	$.1107 \times 10^{-2}$	7, 25	$.2031 \times 10^{-2}$	9, 25	$.3129 \times 10^{-2}$	11, 29	$.4821 \times 10^{-2}$
5, 30	$.1123 \times 10^{-2}$	7, 26	$.2080 \times 10^{-2}$	9, 26	$.3208 \times 10^{-2}$	11, 30	$.4903 \times 10^{-2}$
		7, 27	$.2119 \times 10^{-2}$	9, 27	$.3270 \times 10^{-2}$		
6, 6	0.3361×10^{-3}	7, 28	$.2145 \times 10^{-2}$	9, 28	$.3312 \times 10^{-2}$	12, 12	0.2693×10^{-2}
6, 7	$.4325 \times 10^{-3}$	7, 29	$.2174 \times 10^{-2}$	9, 29	$.3359 \times 10^{-2}$	12, 13	$.3031 \times 10^{-2}$
6, 8	$.5052 \times 10^{-3}$	7, 30	$.2208 \times 10^{-2}$	9, 30	$.3413 \times 10^{-2}$	12, 14	$.3286 \times 10^{-2}$
6, 9	$.5877 \times 10^{-3}$					12, 15	$.3501 \times 10^{-2}$
6, 10	$.6702 \times 10^{-3}$	8, 8	0.8019×10^{-3}	10, 10	0.1557×10^{-2}	12, 16	$.3654 \times 10^{-2}$
6, 11	$.7531 \times 10^{-3}$	8, 9	$.9505 \times 10^{-3}$	10, 11	$.1790 \times 10^{-2}$	12, 17	$.3854 \times 10^{-2}$
6, 12	$.8367 \times 10^{-3}$	8, 10	$.1099 \times 10^{-2}$	10, 12	$.2025 \times 10^{-2}$	12, 18	$.4055 \times 10^{-2}$
6, 13	$.9203 \times 10^{-3}$	8, 11	$.1249 \times 10^{-2}$	10, 13	$.2260 \times 10^{-2}$	12, 19	$.4244 \times 10^{-2}$
6, 14	$.9832 \times 10^{-3}$	8, 12	$.1399 \times 10^{-2}$	10, 14	$.2437 \times 10^{-2}$	12, 20	$.4421 \times 10^{-2}$
6, 15	$.1036 \times 10^{-2}$	8, 13	$.1550 \times 10^{-2}$	10, 15	$.2587 \times 10^{-2}$	12, 21	$.4597 \times 10^{-2}$
6, 16	$.1074 \times 10^{-2}$	8, 14	$.1663 \times 10^{-2}$	10, 16	$.2693 \times 10^{-2}$	12, 22	$.4723 \times 10^{-2}$
6, 17	$.1124 \times 10^{-2}$	8, 15	$.1758 \times 10^{-2}$	10, 17	$.2832 \times 10^{-2}$	12, 23	$.4864 \times 10^{-2}$
6, 18	$.1173 \times 10^{-2}$	8, 16	$.1826 \times 10^{-2}$	10, 18	$.2972 \times 10^{-2}$	12, 24	$.5044 \times 10^{-2}$
6, 19	$.1220 \times 10^{-2}$	8, 17	$.1916 \times 10^{-2}$	10, 19	$.3103 \times 10^{-2}$	12, 25	$.5220 \times 10^{-2}$
6, 20	$.1264 \times 10^{-2}$	8, 18	$.2005 \times 10^{-2}$	10, 20	$.3226 \times 10^{-2}$	12, 26	$.5360 \times 10^{-2}$
6, 21	$.1307 \times 10^{-2}$	8, 19	$.2089 \times 10^{-2}$	10, 21	$.3348 \times 10^{-2}$	12, 27	$.5471 \times 10^{-2}$
6, 22	$.1338 \times 10^{-2}$	8, 20	$.2168 \times 10^{-2}$	10, 22	$.3436 \times 10^{-2}$	12, 28	$.5545 \times 10^{-2}$
6, 23	$.1373 \times 10^{-2}$	8, 21	$.2247 \times 10^{-2}$	10, 23	$.3533 \times 10^{-2}$	12, 29	$.5628 \times 10^{-2}$
6, 24	$.1418 \times 10^{-2}$	8, 22	$.2303 \times 10^{-2}$	10, 24	$.3658 \times 10^{-2}$	12, 30	$.5724 \times 10^{-2}$
6, 25	$.1461 \times 10^{-2}$	8, 23	$.2365 \times 10^{-2}$	10, 25	$.3781 \times 10^{-2}$		

TABLE V.- INFLUENCE COEFFICIENTS – Concluded

i,j	$\sigma_{i,j}$, in./lb	i,j	$\sigma_{i,j}$, in./lb	i,j	$\sigma_{i,j}$, in./lb	i,j	$\sigma_{i,j}$, in./lb
13, 13	0.3427×10^{-2}	15, 25	0.7137×10^{-2}	18, 27	0.9247×10^{-2}	22, 28	0.1205×10^{-1}
13, 14	$.3726 \times 10^{-2}$	15, 26	$.7340 \times 10^{-2}$	18, 28	$.9392 \times 10^{-2}$	22, 29	$.1229 \times 10^{-1}$
13, 15	$.3978 \times 10^{-2}$	15, 27	$.7499 \times 10^{-2}$	18, 29	$.9551 \times 10^{-2}$	22, 30	$.1257 \times 10^{-1}$
13, 16	$.4157 \times 10^{-2}$	15, 28	$.7607 \times 10^{-2}$	18, 30	$.9738 \times 10^{-2}$		
13, 17	$.4393 \times 10^{-2}$	15, 29	$.7726 \times 10^{-2}$			23, 23	0.1053×10^{-1}
13, 18	$.4629 \times 10^{-2}$	15, 30	$.7865 \times 10^{-2}$	19, 19	0.7277×10^{-2}	23, 24	$.1110 \times 10^{-1}$
13, 19	$.4850 \times 10^{-2}$			19, 20	$.7660 \times 10^{-2}$	23, 25	$.1165 \times 10^{-1}$
13, 20	$.5057 \times 10^{-2}$	16, 16	0.5110×10^{-2}	19, 21	$.8043 \times 10^{-2}$	23, 26	$.1209 \times 10^{-1}$
13, 21	$.5265 \times 10^{-2}$	16, 17	$.5422 \times 10^{-2}$	19, 22	$.8315 \times 10^{-2}$	23, 27	$.1244 \times 10^{-1}$
13, 22	$.5412 \times 10^{-2}$	16, 18	$.5734 \times 10^{-2}$	19, 23	$.8620 \times 10^{-2}$	23, 28	$.1268 \times 10^{-1}$
13, 23	$.5577 \times 10^{-2}$	16, 19	$.6028 \times 10^{-2}$	19, 24	$.9009 \times 10^{-2}$	23, 29	$.1294 \times 10^{-1}$
13, 24	$.5788 \times 10^{-2}$	16, 20	$.6303 \times 10^{-2}$	19, 25	$.9391 \times 10^{-2}$	23, 30	$.1324 \times 10^{-1}$
13, 25	$.5995 \times 10^{-2}$	16, 21	$.6577 \times 10^{-2}$	19, 26	$.9696 \times 10^{-2}$		
13, 26	$.6160 \times 10^{-2}$	16, 22	$.6773 \times 10^{-2}$	19, 27	$.9934 \times 10^{-2}$	24, 24	0.1175×10^{-1}
13, 27	$.6289 \times 10^{-2}$	16, 23	$.6991 \times 10^{-2}$	19, 28	$.1010 \times 10^{-1}$	24, 25	$.1239 \times 10^{-1}$
13, 28	$.6377 \times 10^{-2}$	16, 24	$.7271 \times 10^{-2}$	19, 29	$.1027 \times 10^{-1}$	24, 26	$.1291 \times 10^{-1}$
13, 29	$.6473 \times 10^{-2}$	16, 25	$.7545 \times 10^{-2}$	19, 30	$.1048 \times 10^{-1}$	24, 27	$.1331 \times 10^{-1}$
13, 30	$.6586 \times 10^{-2}$	16, 26	$.7764 \times 10^{-2}$			24, 28	$.1359 \times 10^{-1}$
		16, 27	$.7935 \times 10^{-2}$	20, 20	0.8085×10^{-2}	24, 29	$.1389 \times 10^{-1}$
14, 14	0.4060×10^{-2}	16, 28	$.8051 \times 10^{-2}$	20, 21	$.8511 \times 10^{-2}$	24, 30	$.1425 \times 10^{-1}$
14, 15	$.4342 \times 10^{-2}$	16, 29	$.8179 \times 10^{-2}$	20, 22	$.8813 \times 10^{-2}$		
14, 16	$.4543 \times 10^{-2}$	16, 30	$.8329 \times 10^{-2}$	20, 23	$.9151 \times 10^{-2}$	25, 25	0.1316×10^{-1}
14, 17	$.4807 \times 10^{-2}$			20, 24	$.9584 \times 10^{-2}$	25, 26	$.1378 \times 10^{-1}$
14, 18	$.5070 \times 10^{-2}$	17, 17	0.5768×10^{-2}	20, 25	$.1001 \times 10^{-1}$	25, 27	$.1426 \times 10^{-1}$
14, 19	$.5318 \times 10^{-2}$	17, 18	$.6116 \times 10^{-2}$	20, 26	$.1035 \times 10^{-1}$	25, 28	$.1459 \times 10^{-1}$
14, 20	$.5550 \times 10^{-2}$	17, 19	$.6442 \times 10^{-2}$	20, 27	$.1061 \times 10^{-1}$	25, 29	$.1495 \times 10^{-1}$
14, 21	$.5782 \times 10^{-2}$	17, 20	$.6748 \times 10^{-2}$	20, 28	$.1079 \times 10^{-1}$	25, 30	$.1537 \times 10^{-1}$
14, 22	$.5948 \times 10^{-2}$	17, 21	$.7053 \times 10^{-2}$	20, 29	$.1099 \times 10^{-1}$		
14, 23	$.6132 \times 10^{-2}$	17, 22	$.7271 \times 10^{-2}$	20, 30	$.1122 \times 10^{-1}$	26, 26	0.1450×10^{-1}
14, 24	$.6368 \times 10^{-2}$	17, 23	$.7514 \times 10^{-2}$			26, 27	$.1509 \times 10^{-1}$
14, 25	$.6600 \times 10^{-2}$	17, 24	$.7825 \times 10^{-2}$	21, 21	0.8983×10^{-2}	26, 28	$.1549 \times 10^{-1}$
14, 26	$.6784 \times 10^{-2}$	17, 25	$.8130 \times 10^{-2}$	21, 22	$.9319 \times 10^{-2}$	26, 29	$.1593 \times 10^{-1}$
14, 27	$.6929 \times 10^{-2}$	17, 26	$.8373 \times 10^{-2}$	21, 23	$.9695 \times 10^{-2}$	26, 30	$.1645 \times 10^{-1}$
14, 28	$.7027 \times 10^{-2}$	17, 27	$.8563 \times 10^{-2}$	21, 24	$.1018 \times 10^{-1}$		
14, 29	$.7135 \times 10^{-2}$	17, 28	$.8692 \times 10^{-2}$	21, 25	$.1065 \times 10^{-1}$	27, 27	0.1582×10^{-1}
14, 30	$.7262 \times 10^{-2}$	17, 29	$.8835 \times 10^{-2}$	21, 26	$.1102 \times 10^{-1}$	27, 28	$.1632 \times 10^{-1}$
		17, 30	$.9002 \times 10^{-2}$	21, 27	$.1132 \times 10^{-1}$	27, 29	$.1687 \times 10^{-1}$
15, 15	0.4652×10^{-2}			21, 28	$.1152 \times 10^{-1}$	27, 30	$.1751 \times 10^{-1}$
15, 16	$.4873 \times 10^{-2}$	18, 18	0.6504×10^{-2}	21, 29	$.1174 \times 10^{-1}$		
15, 17	$.5163 \times 10^{-2}$	18, 19	$.6870 \times 10^{-2}$	21, 30	$.1200 \times 10^{-1}$	28, 28	0.1689×10^{-1}
15, 18	$.5453 \times 10^{-2}$	18, 20	$.7212 \times 10^{-2}$			28, 29	$.1752 \times 10^{-1}$
15, 19	$.5726 \times 10^{-2}$	18, 21	$.7555 \times 10^{-2}$	22, 22	0.9681×10^{-2}	28, 30	$.1825 \times 10^{-1}$
15, 20	$.5982 \times 10^{-2}$	18, 22	$.7799 \times 10^{-2}$	22, 23	$.1009 \times 10^{-1}$		
15, 21	$.6237 \times 10^{-2}$	18, 23	$.8071 \times 10^{-2}$	22, 24	$.1060 \times 10^{-1}$	29, 29	0.1823×10^{-1}
15, 22	$.6419 \times 10^{-2}$	18, 24	$.8420 \times 10^{-2}$	22, 25	$.1111 \times 10^{-1}$	29, 30	$.1907 \times 10^{-1}$
15, 23	$.6622 \times 10^{-2}$	18, 25	$.8761 \times 10^{-2}$	22, 26	$.1152 \times 10^{-1}$		
15, 24	$.6882 \times 10^{-2}$	18, 26	$.9034 \times 10^{-2}$	22, 27	$.1184 \times 10^{-1}$	30, 30	0.2010×10^{-1}